Incremental Model Predictive Control Exploiting Time-Delay Estimation for a Robot Manipulator

Wang, Yongchao; Leibold, Marion; Lee, Jinoh; Ye, Wenyan; Xie, Jing; Buss, Martin

Incremental Model Predictive Control Exploiting Time-Delay Estimation for a Robot Manipulator

Yongchao Wang, Marion Leibold, *Member, IEEE*, Jinoh Lee, *Senior Member, IEEE*, Wenyan Ye, Jing Xie, *Graduate Student Member, IEEE*, and Martin Buss, *Fellow, IEEE*

***Abstract*— This article proposes a new incremental model predictive control (IMPC) strategy, which allows for constrained control of a robot manipulator, while the resulting incremental model is derived without a concrete mathematical system model. First, to reduce dependence on the nominal model of robot manipulators, the continuous-time nonlinear system model is approximated by an incremental system using the time-delay estimation (TDE). Then, based on the incremental system, the tracking IMPC is designed in the framework of MPC without terminal ingredients. Thus, compared with existing MPC methods, the nominal mathematical model is not required. Moreover, we investigate reachable reference trajectories and confirm the local input-to-state stability (ISS) of IMPC, considering the bounded TDE error as the disturbance of the incremental system. For reachable reference trajectories, the local ISS of IMPC is analyzed using the continuity of the value function, and the cumulative error bound is not overconservative. Finally, several real-time experiments are conducted to verify the effectiveness of IMPC. Experimental results show that the system can achieve optimal control performance while guaranteeing that input and state constraints are not violated.**

***Index Terms*— Incremental system, input-to-state stability (ISS), model predictive control (MPC), time-delay estimation (TDE).**

NOMENCLATURE

$\mathbb{R}$, $\mathbb{R}_{\geq 0}$, and $\mathbb{R}_{>0}$	Real, nonnegative, and positive sets.
$\mathbb{I}$ and $\mathbb{I}_{>0}$	Integer and positive integer sets.
$\mathbb{I}_{[a,b]}$	$\mathbb{I}_{[a,b]} = \{x \in \mathbb{I} : a \leq x \leq b\}$.
$\lceil x \rceil \in \mathbb{I}$	Smallest integer greater than $x \in \mathbb{R}$.
$\mathbf{I}, \mathbf{O}, \mathbf{0}$	Identity matrix, null matrix, and null vector.
$\text{col}(\mathbf{x}_1, \mathbf{x}_2)$	Column vectors of $\mathbf{x}_1$ and $\mathbf{x}_2$, $[\mathbf{x}_1^\top, \mathbf{x}_2^\top]^\top$.
$\mathbf{Q} \succ 0$	Positive-definite matrix $\mathbf{Q}$.
$\|\bullet\|$	Euclidean norm of $\bullet$.
$\|\mathbf{x}\|_\mathbf{Q}$	$\|\mathbf{x}\|_\mathbf{Q} = \sqrt{\mathbf{x}^\top \mathbf{Q} \mathbf{x}}$ for $\mathbf{x}$ and $\mathbf{Q} \succ 0$.
$\lambda(\mathbf{Q})$	Eigenvalue of $\mathbf{Q}$.
$\lambda_{\min}$ and $\lambda_{\max}$	Minimal and maximal eigenvalues.

A continuous function $\alpha : [0, a) \to \mathbb{R}_{\geq 0}$, for some $a > 0$, is said to belong to class $\mathcal{K}$ if it is zero at zero and strictly increasing. Moreover, $\alpha(\cdot)$ is said to belong to class $\mathcal{K}_\infty$ if it is a class $\mathcal{K}$ function with $a = \infty$ and radially unbounded, i.e., $\alpha(x) \to \infty$ as $x \to \infty$. A continuous function $\sigma : \mathbb{R}_{>0} \to \mathbb{R}_{\geq 0}$ is said to belong to class $\mathcal{L}$ if it decreases with $\lim_{k \to \infty} \sigma(k) = 0$. A continuous function $\beta : [0, a) \times [0, \infty) \to [0, \infty)$ is said to belong to class $\mathcal{KL}$ if, for each fixed s, the mapping $\beta(r, s)$ belongs to class $\mathcal{K}$ with respect to r and, for each fixed r, the mapping $\beta(r, s)$ belongs to class $\mathcal{L}$. If $\mathbb{S}_1$, $\mathbb{S}_2$, and $\mathbb{S}_3$ are any sets and $f_1 : \mathbb{S}_1 \to \mathbb{S}_2$ and $f_2 : \mathbb{S}_2 \to \mathbb{S}_3$ are functions, then the function $f_2 \circ f_1 : \mathbb{S}_1 \to \mathbb{S}_3$, defined by $(f_2 \circ f_1)(\cdot) = f_2(f_1(\cdot))$, is called the composition of f_1 and f_2.

Manuscript received October 21, 2021; accepted December 17, 2021. This work was supported in part by the National Science Foundation of China under Grant 61673308 and in part by the ITECH Research and Development Programs of Ministry of Trade, Industry and Energy (MOTIE)/Korea Evaluation Institute of Industrial Technology (KEIT) under Project 20014398 and Project 20014485. Recommended by Associate Editor Y. Pan. *(Corresponding author: Jinoh Lee.)*

Yongchao Wang, Marion Leibold, Jing Xie, and Martin Buss are with the Chair of Automatic Control Engineering (LSR), Technical University of Munich, 80333 Munich, Germany (e-mail: yongchao.wang@tum.de; marion.leibold@tum.de; jing.xie@tum.de; mb@tum.de).

Jinoh Lee is with the Institute of Robotics and Mechatronics, German Aerospace Center (DLR), 82234 Weßling, Germany (e-mail: jinoh.lee@dlr.de).

Wenyan Ye was with the Chair of Automatic Control Engineering (LSR), Technical University of Munich, 80333 Munich, Germany. He is now with the Institute of Automatic Control, University of Kaiserslautern, 67653 Kaiserslautern, Germany (e-mail: ye@eit.uni-kl.de).

Color versions of one or more figures in this article are available at https://doi.org/10.1109/TCST.2022.3142629.

Digital Object Identifier 10.1109/TCST.2022.3142629

I. INTRODUCTION

THE major challenge in robot manipulator control, e.g., in manufacturing [1] or aerospace applications [2], is to be able to accurately track reference trajectories in joint or task space. In the last few decades, robustness properties of these controllers have been intensively investigated to deal with uncertainty and external disturbances [3]. Nevertheless, optimality of controllers and accounting for input and state constraints was not yet thoroughly addressed together, while constraints can be used to describe safety requirements on control and thus enable robot manipulators to also be used in safety-critical applications, e.g., close to or in cooperation with humans.

A. Related Works

Nonlinear control approaches, such as computed torque [4] or backstepping [5], are able to deliver high-performance controllers for robot manipulators. However, a precise model is needed and performance is deteriorated in the presence of model uncertainties and disturbances. To address the robustness issue, disturbance observers [6], sliding mode controllers (SMCs) [7], [8], and adaptive control methods [9]

are employed and often combined with computed torque or backstepping. Nevertheless, the nominal model of the robot manipulator and its parameters still need to be identified. To alleviate the need of concrete mathematical modeling and parameter identification, intelligent control techniques, such as fuzzy logic systems [10] and neural networks (NNs) [11], are proposed to approximate unknown/uncertain system dynamics. Yet, these approaches also pay more attention to robustness, not to optimal tracking performance. In addition, input and state constraints are usually not of interest.

Model predictive control (MPC) [12], or receding horizon control [13], is an optimization-based control addressing optimal tracking control performance and input and state constraints, such as saturation of control inputs and physical limits of workspace and speed. The distinct feature of MPC lies in its capability of systematically handling input and state constraints within the controller design. For MPC, the constrained optimal control problem (OCP) is solved using the state predictions generated by the nominal mathematical model in a horizon [14]–[18], where the difference between the nominal and real mathematical models due to uncertainties and disturbances may degrade tracking performance [19]. Besides, when some dynamics terms are unknown, MPC algorithms in [14]–[19] are not able to be implemented.

A robust MPC was proposed for a helicopter in [20] where an extended high-gain observer estimates model uncertainties and disturbances. However, the nominal mathematical model is required. Learning-based MPC methods are proposed [21]–[23] to deal with uncertain/unknown system dynamics, where Gaussian process (GP) and NNs are used to identify nonlinear models online, which can reduce dependence on the concrete mathematical model. A data-driven MPC was developed in [24], where a nonparametric machine learning technique is used to estimate a prediction model. Unfortunately, learning and data-driven techniques further increase the computational complexity of MPC. Other robust MPC schemes, including min-max optimization [25], [26] and sliding mode techniques [27], [28], are also employed to improve robustness without significant increase of complexities. Alternatively, MPC is formulated with an incremental model, which generates the state predictions by using both present and previous states [29]. However, since the incremental system is obtained from linearization of the nonlinear system, the controller is effective only locally around equilibrium points.

Model uncertainties and disturbances not only increase the computational complexity of MPC, but they also make stability analysis more challenging. Due to uncertainties and/or disturbances, the Lyapunov stability that was established for the nominal system is not simply transferable [17], [18], and input-to-state stability (ISS), also known as practical Lyapunov stability, is required to be considered. In [30] and [31], ISS of MPC with terminal ingredients was analyzed where a feasible control sequence, which guarantees that input and state constraints are not violated, was employed. However, the derived cumulative error bound increases with increasing the prediction horizon. It results in an overconservative cumulative error bound, which conveys that the tracking error increases for increasing the prediction horizon. However, in practice, increasing prediction horizon appropriately will decrease tracking errors [32]. Thus, the derived overconservative cumulative error bound provides a wrong guidance to improve tracking accuracy.

For MPC without terminal ingredients, the ISS property was investigated in [33], where time-variant sets of admissible predicted states are used. In [34] and [35], for linear systems, the continuity property of the value function was applied to estimate cumulative error bounds and then verify ISS. Feasible control sequences were not required and time-invariant input and state constraints could be used. Unfortunately, if the eigenvalue of the system matrix (also known as coefficient matrix) is greater than one, it still results in the rise of the cumulative error bound with increasing the prediction horizon.

B. Method and Contributions

In this article, an incremental model predictive control (IMPC) method is developed for a robot manipulator modeled by Euler–Lagrange equations. To obtain optimal performance in the presence of input and state constraints as well as the robustness against uncertainties and disturbances, we first design a robust incremental model in the global set of admissible states exploiting the time-delay estimation (TDE) technique [36], [37]. TDE is a model-free method, which uses time-delayed input and output signals to estimate partial dynamics of the system without concrete mathematical model, laborious parameter identification, and linearization around equilibrium points of the system [38]–[40]. Then, an MPC problem is formulated, where the state predictions are generated from the discretized incremental control system derived by TDE.

In particular, a reachable reference trajectory is defined, for which ISS of the proposed IMPC is analyzed. Using continuity of the value function, ISS is verified and overconservative cumulative error bound is avoided. ISS is shown for all horizon lengths that are larger than a specific threshold derived recursively. The contributions are summarized as follows.

1) *No Concrete Mathematical Model Required:* Different from existing MPC methods, the concrete mathematical model of the robot manipulator is not required. This is because the continuous-time nonlinear system model is approximated by an incremental system using TDE, and the state predictions are generated using the linear discretized incremental system.
2) *Optimal Performance for TDE-Based Control:* The TDE-based incremental controller is developed in the framework of MPC without terminal ingredients, and input and state constraints are formulated as inequality constraints. Thus, optimal control performance is achieved, while input and state constraints are considered, which has not been considered in existing TDE-based controllers [36]–[40].
3) *No Overconservative Cumulative Error Bound:* Considering the bounded error sourced from TDE as the major disturbance, local ISS of IMPC is confirmed. Different from existing ISS analyses for MPC, here, continuity of the value function is used to derive the upper bound

of the difference between two value functions, and the resulting cumulative error bound is not overconservative. It is theoretically inferred from this ISS and the cumulative error bound that increasing the prediction horizon enlarges the region of attraction and, at the same time, decreases tracking errors.

C. Organization

The rest of this article is organized as follows. In Section II, the robot manipulator dynamics is introduced, and the nonlinear system is approximated by an incremental system using TDE. Section III presents the proposed IMPC. The local ISS property of IMPC is theoretically analyzed in Section IV. A series of real-time experiments is performed on a robot manipulator and the effectiveness of the proposed IMPC is verified in Section V followed by a conclusion in Section VI.

II. Incremental System With TDE

A. Robot Manipulator Dynamics

The model of an n-link robot manipulator is given as [41]

$$\mathbf{M}(\mathbf{q})\ddot{\mathbf{q}} + \mathbf{C}(\mathbf{q}, \dot{\mathbf{q}})\dot{\mathbf{q}} + \mathbf{G}(\mathbf{q}) + \mathbf{F}(\dot{\mathbf{q}}) = \boldsymbol{\tau} \tag{1}$$

where $\mathbf{q}, \dot{\mathbf{q}}, \ddot{\mathbf{q}} \in \mathbb{R}^n$ represent the position, velocity, and acceleration of joints, respectively, $\mathbf{M}(\mathbf{q}) \in \mathbb{R}^{n\times n}$ is the symmetric inertia matrix, $\mathbf{C}(\mathbf{q}, \dot{\mathbf{q}}) \in \mathbb{R}^{n\times n}$ is the Coriolis/centrifugal matrix, $\mathbf{G}(\mathbf{q}) \in \mathbb{R}^n$ contains the gravitational terms exerting on the robot manipulator, $\mathbf{F}(\dot{\mathbf{q}}) \in \mathbb{R}^n$ denotes viscous friction, and $\boldsymbol{\tau} \in \mathbb{R}^n$ is the vector of torque supplied by the actuators. The Euler–Lagrange system (1) satisfies the following property.

Property 1 [42]: The inertia matrix $\mathbf{M}(\mathbf{q})$ is uniformly positive definite and there exist constants μ_1, $\mu_2 \in \mathbb{R}_{>0}$ such that each eigenvalue of $\mathbf{M}(\mathbf{q})$, denoted by $\lambda_i(\mathbf{M}(\mathbf{q}))$, satisfies

$$\mu_1 \le \lambda_i(\mathbf{M}(\mathbf{q})) \le \mu_2 \quad \forall i \in \mathbb{I}_{[1,n]}.$$

If $[\mathbf{x}_1, \mathbf{x}_2] := [\mathbf{q}, \dot{\mathbf{q}}]$ and $\mathbf{u} := \boldsymbol{\tau}$, then (1) is rewritten as a second-order nonlinear system in a strict-feedback form

$$\dot{\mathbf{x}}_1 = \mathbf{x}_2, \tag{2a}$$

$$\dot{\mathbf{x}}_2 = \mathbf{f}(\mathbf{x}) + \mathbf{g}(\mathbf{x})\mathbf{u} \tag{2b}$$

where $\mathbf{f}(\mathbf{x}) := -\mathbf{M}^{-1}(\mathbf{q})(\mathbf{C}(\mathbf{q}, \dot{\mathbf{q}})\dot{\mathbf{q}} + \mathbf{G}(\mathbf{q}) + \mathbf{F}(\dot{\mathbf{q}}))$, $\mathbf{g}(\mathbf{x}) := \mathbf{M}^{-1}(\mathbf{q})$, and $\mathbf{x} := \mathrm{col}(\mathbf{x}_1, \mathbf{x}_2)$.

According to [8] and [43], $\mathbf{M}(\mathbf{q})$, $\mathbf{C}(\mathbf{q}, \dot{\mathbf{q}})$, $\mathbf{G}(\mathbf{q})$, and $\mathbf{F}(\dot{\mathbf{q}})$ are all upper bounded. Thus, the following assumption is made for $\mathbf{f}(\mathbf{x})$ in an admissible set $\mathbb{D}_{\mathbf{x}} \subset \mathbb{R}^{2n}$.

Assumption 1: $\mathbf{f}(\mathbf{x})$ with $\mathbf{f}(\mathbf{0}) = \mathbf{0}$ is upper bounded in $\mathbb{D}_{\mathbf{x}}$, with constants $f_{\max}$, $f_0 \in \mathbb{R}_{>0}$, i.e.,

$$\|\mathbf{f}(\mathbf{x})\| \le f_{\max}\|\mathbf{x}\| + f_0 \quad \forall \mathbf{x} \in \mathbb{D}_{\mathbf{x}}. \tag{3}$$

Note that $\mathbf{M}(\mathbf{q})$, $\mathbf{C}(\mathbf{q}, \dot{\mathbf{q}})$, $\mathbf{G}(\mathbf{q})$, and $\mathbf{F}(\dot{\mathbf{q}})$ are unknown/uncertain because of unmodeled dynamics, disturbances, and time-varying friction. Therefore, parameters of $\mathbf{f}(\mathbf{x})$ and $\mathbf{g}(\mathbf{x})$ are considered to be unknown in this article.

B. Derivation of the TDE-Based Incremental System

The TDE technique [36], [37] is employed to approximate the nonlinear system model and then acquire the incremental system. Following the presentation in [44], an approximation of the current system dynamic behavior is found from monitoring the most recent states and control inputs. A linear system model with an incremental control signal is derived.

Introducing a constant positive-definite diagonal matrix $\bar{\mathbf{g}}$, (2b) is reformulated as follows:

$$\bar{\mathbf{g}}^{-1}\dot{\mathbf{x}}_2 = \mathbf{H}(\mathbf{x}, \dot{\mathbf{x}}) + \mathbf{u} \tag{4}$$

where $\mathbf{H}(\mathbf{x}, \dot{\mathbf{x}}) := \big(\bar{\mathbf{g}}^{-1} - \mathbf{g}^{-1}(\mathbf{x})\big)\dot{\mathbf{x}}_2 + \mathbf{g}^{-1}(\mathbf{x})\mathbf{f}(\mathbf{x})$, which includes all uncertain/unknown model dynamics. For a sufficiently small L, the value of $\mathbf{H}(\mathbf{x}, \dot{\mathbf{x}})$ at time t is close to that of $\mathbf{H}(\mathbf{x}, \dot{\mathbf{x}})$ at time $(t - L)$ [44]

$$\mathbf{H}(\mathbf{x}, \dot{\mathbf{x}})_{(t)} \cong \mathbf{H}(\mathbf{x}, \dot{\mathbf{x}})_{(t-L)}. \tag{5}$$

Abbreviating $\dot{\mathbf{x}}_{2,0} := (\dot{\mathbf{x}}_2)_{(t-L)}$ and $\mathbf{u}_0 := \mathbf{u}_{(t-L)}$ yields

$$\mathbf{H}(\mathbf{x}, \dot{\mathbf{x}})_{(t-L)} = \bar{\mathbf{g}}^{-1}\dot{\mathbf{x}}_{2,0} - \mathbf{u}_0. \tag{6}$$

From (5) and (6), one obtains the TDE of $\mathbf{H}(\mathbf{x}, \dot{\mathbf{x}})$, i.e., $\hat{\mathbf{H}}(\mathbf{x}, \dot{\mathbf{x}})$ as follows [36]–[40], [44], [45]:

$$\hat{\mathbf{H}}(\mathbf{x}, \dot{\mathbf{x}}) = \mathbf{H}(\mathbf{x}, \dot{\mathbf{x}})_{(t-L)} = \bar{\mathbf{g}}^{-1}\dot{\mathbf{x}}_{2,0} - \mathbf{u}_0. \tag{7}$$

From (7), one learns that, to obtain $\hat{\mathbf{H}}(\mathbf{x}, \dot{\mathbf{x}})$, the most recent values $\dot{\mathbf{x}}_{2,0}$ and $\mathbf{u}_0$ are required instead of the complex and uncertain robot dynamics. Thus, with the combination of (4), (6) and (7), an incremental version of (2b) is obtained

$$\dot{\mathbf{x}}_2 = \dot{\mathbf{x}}_{2,0} + \bar{\mathbf{g}}(\Delta\mathbf{u} + \boldsymbol{\epsilon}) \tag{8}$$

where $\Delta\mathbf{u} := \mathbf{u} - \mathbf{u}_0$ is the incremental control signal and $\boldsymbol{\epsilon} := \mathbf{H}(\mathbf{x}, \dot{\mathbf{x}}) - \hat{\mathbf{H}}(\mathbf{x}, \dot{\mathbf{x}})$ is the TDE error acting as disturbances to the incremental system.

To avoid significant mismatch between $\mathbf{g}(\mathbf{x})$ and $\bar{\mathbf{g}}$, $\bar{\mathbf{g}}$ is selected such that $\|\mathbf{I} - \mathbf{g}(\mathbf{x})\bar{\mathbf{g}}^{-1}\| < 1$ in this article and the boundedness property analysis for the TDE error $\boldsymbol{\epsilon}$ is given in Lemma 3.

Remark 1: For a specific robot manipulator, the principle to determine the diagonal matrix $\bar{\mathbf{g}}$ is presented as follows. According to Property 1, $\lambda_i(\mathbf{g}(\mathbf{x}))$ is bounded by $0 < (1/\mu_2) \le \lambda_i(\mathbf{g}(\mathbf{x})) \le (1/\mu_1)$ since $\mathbf{g}(\mathbf{x}) = \mathbf{M}^{-1}(\mathbf{q})$. Suppose that $\bar{g}_i$ is the ith diagonal element of $\bar{\mathbf{g}}$, and then, $\forall i \in \mathbb{I}_{[1,n]}$, $(1 - (\lambda_i/\bar{g}_i))$ is an eigenvalue of $(\mathbf{I} - \mathbf{g}(\mathbf{x})\bar{\mathbf{g}}^{-1})$. If $|1 - (\lambda_i/\bar{g}_i)| < 1$, i.e., $\bar{g}_i$ satisfies $\bar{g}_i > (\lambda_i/2)$, then $\|\mathbf{I} - \mathbf{g}(\mathbf{x})\bar{\mathbf{g}}^{-1}\| < 1$ holds. This also implies that the sufficient condition for $\|\mathbf{I} - \mathbf{g}(\mathbf{x})\bar{\mathbf{g}}^{-1}\| < 1$ can be achieved by large positive $\bar{g}_i$ although exact expressions and eigenvalues of $\mathbf{g}(\mathbf{x})$ are unknown [39].

III. Reference Tracking Incremental MPC

In this section, the control objective is first introduced, which is a prerequisite to formulate the MPC problem. Then, discretizing the incremental system derived by TDE, an approximated discrete-time linear system is obtained. Based on the approximated discrete-time linear system, the reference tracking IMPC is developed through formulating a constrained OCP.

A. Control Objective

The control objective is to make the robot manipulator track the given reference signal $\mathbf{x}_{\text{ref}}$ and impose the following point-wise constraints on state and input:

$$(\mathbf{x}, \mathbf{u}) \in \mathbb{Z} = \mathbb{X} \times \mathbb{U} \tag{9}$$

where $\mathbb{X}$, $\mathbb{U}$, and $\mathbb{Z}$ are all compact sets containing the origin in their interior.

Constraints are imposed on state and input in (9), i.e., $\mathbf{x} \in \mathbb{X}$, and $\mathbf{u} \in \mathbb{U}$. In the context of the robot manipulator, the joint position, velocity, and torque are constrained by $|q_i| \leq q_{i,\max}$, $|\dot{q}_i| \leq \dot{q}_{i,\max}$, and $|\tau_i| \leq \tau_{i,\max}$ with $q_{i,\max}, \dot{q}_{i,\max}$, and $\tau_{i,\max} \in \mathbb{R}_{>0}$ being specified limits.

In this article, only smooth reference trajectories $\mathbf{x}_{\text{ref}}$ are considered since nonsmooth reference trajectories can cause damage to mechanical systems due to sharp actuator changes. Without loss of generality, reference trajectories are assumed to be smooth and bounded.

Assumption 2 [46]: The joint position reference signal $\mathbf{q}_{\text{ref}}$ is smooth and bounded, satisfying $0 \leq \underline{r} \leq \|\mathbf{q}_{\text{ref}}\| \leq \overline{r} < \infty$, $0 \leq \underline{\dot{r}} \leq \|\dot{\mathbf{q}}_{\text{ref}}\| \leq \overline{\dot{r}} < \infty$, and $0 \leq \underline{\ddot{r}} \leq \|\ddot{\mathbf{q}}_{\text{ref}}\| \leq \overline{\ddot{r}} < \infty$.

Note that according to the definition in (2), the reference signal $\mathbf{x}_{\text{ref}} := \left(\mathbf{x}_{1,\text{ref}}, \mathbf{x}_{2,\text{ref}}\right) := (\mathbf{q}_{\text{ref}}, \dot{\mathbf{q}}_{\text{ref}})$.

B. Formulation of the Proposed IMPC

In this section, the IMPC is developed. First, a discrete-time linear system is obtained by discretizing the incremental system (8) derived by TDE.

Discretizing (2a) and (8) using the following Euler numerical differentiation:

$$\dot{\mathbf{x}}_*(k) = \frac{\mathbf{x}_*(k+1) - \mathbf{x}_*(k)}{T_s} + \boldsymbol{\omega}_*(k)$$

where $\boldsymbol{\omega}_*(k)$ is the dicretization error. Replacing $\dot{\mathbf{x}}_1$, $\dot{\mathbf{x}}_2$, and $\dot{\mathbf{x}}_{2,0}$ by $\dot{\mathbf{x}}_1(k)$, $\dot{\mathbf{x}}_2(k)$, and $\dot{\mathbf{x}}_2(k-1)$, respectively, and (2) is transformed into the discrete-time form

$$\begin{aligned}\mathbf{x}_1(k+1) &= \mathbf{x}_1(k) + T_s\mathbf{x}_2(k) - T_s\boldsymbol{\omega}_1(k)\\ \mathbf{x}_2(k+1) &= 2\mathbf{x}_2(k) - \mathbf{x}_2(k-1) + \bar{\mathbf{g}}T_s(\Delta\mathbf{u}(k) + \boldsymbol{\epsilon}) + T_s\bar{\boldsymbol{\omega}}_2(k)\end{aligned} \tag{10}$$

where $\bar{\boldsymbol{\omega}}_2(k) := \boldsymbol{\omega}_2(k-1) - \boldsymbol{\omega}_2(k)$ and T_s is the sampling period. Note that it is reasonable to assume that discretization errors are bounded, and the smaller T_s, the smaller are discretization errors.

If $\mathbf{x}(k) := \text{col}(\mathbf{x}_1(k), \mathbf{x}_2(k))$, then (10) is rewritten as

$$\mathbf{x}(k+1) = \mathbf{A}_1\mathbf{x}(k) + \mathbf{A}_2\mathbf{x}(k-1) + \mathbf{B}_1\Delta\mathbf{u}(k) + \bar{\boldsymbol{\epsilon}}_1 \tag{11}$$

with $\mathbf{A}_1 := \begin{bmatrix}\mathbf{I} & T_s\mathbf{I}\\ \mathbf{O} & 2\mathbf{I}\end{bmatrix}$, $\mathbf{A}_2 := \begin{bmatrix}\mathbf{O} & \mathbf{O}\\ \mathbf{O} & -\mathbf{I}\end{bmatrix}$, $\mathbf{B}_1 := \begin{bmatrix}\mathbf{O}\\ \bar{\mathbf{g}}T_s\end{bmatrix}$, and $\bar{\boldsymbol{\epsilon}}_1 := \begin{bmatrix}-T_s\boldsymbol{\omega}_1(k)\\ \bar{\mathbf{g}}T_s\boldsymbol{\epsilon} + T_s\bar{\boldsymbol{\omega}}_2(k)\end{bmatrix}$.

If $\mathbf{X}(k) := \text{col}(\mathbf{x}(k), \mathbf{x}(k-1))$, (11) is then rewritten as a first-order discrete-time system with disturbance $\bar{\boldsymbol{\epsilon}}_2$ given by

$$\mathbf{X}(k+1) = \mathbf{A}\mathbf{X}(k) + \mathbf{B}\Delta\mathbf{u}(k) + \bar{\boldsymbol{\epsilon}}_2 \tag{12}$$

where $\mathbf{A} := \begin{bmatrix}\mathbf{A}_1 & \mathbf{A}_2\\ \mathbf{I} & \mathbf{O}\end{bmatrix}$, $\mathbf{B} := \begin{bmatrix}\mathbf{B}_1\\ \mathbf{O}\end{bmatrix}$, and $\bar{\boldsymbol{\epsilon}}_2 := \begin{bmatrix}\bar{\boldsymbol{\epsilon}}_1\\ \mathbf{O}\end{bmatrix}$.

For $\bar{\boldsymbol{\epsilon}}_2 = \mathbf{0}$, we obtain the nominal system of (12), a discrete-time linear system

$$\mathbf{X}(k+1) = \mathbf{A}\mathbf{X}(k) + \mathbf{B}\Delta\mathbf{u}(k). \tag{13}$$

Note that the linear system $(\mathbf{A}, \mathbf{B})$ is controllable. Different from conventional linearization methods, such as Taylor series [29], [47] and Carleman approaches [48], the linear system (13) is obtained without concrete mathematical model. Besides, it is effective in the whole set $\mathbb{D}_{\mathbf{x}}$, not only locally around equilibrium points.

Then, the stage cost function will be defined in the following. Besides $\mathbf{x}_{\text{ref}}$, the reference control signal $\mathbf{u}_{\text{ref}}$ is required to define a reference tracking stage cost function. For nonlinear MPC [49], [50], $\mathbf{u}_{\text{ref}}$ is usually calculated from the nominal model. Since it is assumed that prior knowledge of the nominal model is not available (see Section II-A), the discrete-time linear approximation (13) is used to calculate an approximated incremental reference control signal $\Delta\hat{\mathbf{u}}_{\text{ref}}(k)$

$$\Delta\hat{\mathbf{u}}_{\text{ref}}(k) = \mathbf{B}^{\dagger}(\mathbf{X}_{\text{ref}}(k+1) - \mathbf{A}\mathbf{X}_{\text{ref}}(k)) \tag{14}$$

where $\mathbf{B}^{\dagger} := (\mathbf{B}^{\top}\mathbf{B})^{-1}\mathbf{B}^{\top}$ and $\mathbf{X}_{\text{ref}}(k) := \text{col}(\mathbf{x}_{\text{ref}}(k), \mathbf{x}_{\text{ref}}(k-1))$.

Consider that the full reference trajectory of the manipulator is predefined. The reference trajectories over a finite horizon after time instance k are thus priorly known, and the tracking stage cost function is defined as follows:

$$\begin{aligned}&\ell(\mathbf{X}_{k+i|k}, \Delta\mathbf{u}_{k+i|k}, k+i)\\ &\quad = \|\mathbf{X}_{k+i|k} - \mathbf{X}_{\text{ref}}(k+i)\|^2_{\mathbf{Q}} + \|\Delta\mathbf{u}_{k+i|k} - \Delta\hat{\mathbf{u}}_{\text{ref}}(k+i)\|^2_{\mathbf{R}}\end{aligned} \tag{15}$$

where $\mathbf{Q} \succ 0$ and $\mathbf{R} \succ 0$ are weighting matrices and $\bullet_{k+i|k}$ denotes predictions of states and control inputs, in particular, $\mathbf{X}_{k|k} = \mathbf{X}(k)$, and $\mathbf{X}_{k+i|k}$ is calculated using (13), i.e.,

$$\mathbf{X}_{k+i|k} = \mathbf{A}\mathbf{X}_{k+i-1|k} + \mathbf{B}\Delta\mathbf{u}_{k+i-1|k}. \tag{16}$$

Based on the stage cost function (15), the cost function $J_N(\mathbf{X}(k), \Delta\bar{\mathbf{u}}(k), k) : \mathbb{R}^{4n} \times \mathbb{R}^{n\times N} \times \mathbb{I}_{\geq 0} \to \mathbb{R}$ with respect to an input sequence $\Delta\bar{\mathbf{u}}(k) := [\Delta\mathbf{u}_{k|k}, \ldots, \Delta\mathbf{u}_{k+N-1|k}]$ at time k is defined as follows:

$$\begin{aligned}&J_N(\mathbf{X}(k), \Delta\bar{\mathbf{u}}(k), k)\\ &\quad = \sum_{i=0}^{N-1}\ell(\mathbf{X}_{k+i|k}, \Delta\mathbf{u}_{k+i|k}, k+i) && \text{(17a)}\\ &\qquad \text{s.t. } \mathbf{X}_{k+i+1|k} = \mathbf{A}\mathbf{X}_{k+i|k} + \mathbf{B}\Delta\mathbf{u}_{k+i|k}, && \text{(17b)}\\ &\qquad \mathbf{u}_{k+i+1|k} = \left(\mathbf{u}(k) + \sum_{m=0}^{i}\Delta\mathbf{u}_{k+m|k}\right) \in \mathbb{U} && \text{(17c)}\\ &\qquad \mathbf{X}_{k+i|k} \in \bar{\mathbb{X}} && \text{(17d)}\end{aligned}$$

where $\bar{\mathbb{X}} := \{\mathbf{X} = \text{col}(\mathbf{x}', \mathbf{x}'') \in \mathbb{R}^{4n} : \mathbf{x}' \in \mathbb{X}, \mathbf{x}'' \in \mathbb{X}\}$, $i \in \mathbb{I}_{[0,N-1]}$, and $N \in \mathbb{I}_{>0}$ is the prediction horizon.

Finally, the IMPC is developed in the framework of MPC without terminal ingredients, i.e., the reference tracking IMPC is developed through formulating the following constrained OCP:

$$V_N(\mathbf{X}(k), k) = \min_{\Delta\bar{\mathbf{u}}(k)} J_N(\mathbf{X}(k), \Delta\bar{\mathbf{u}}(k), k). \tag{18}$$

The solution to OCP (18) is an optimal state and input sequence $(\bar{\mathbf{X}}^*_k, \Delta\bar{\mathbf{u}}^*_k)$, where $\bar{\mathbf{X}}^*_k := [\mathbf{X}^*_{k|k}, \ldots, \mathbf{X}^*_{k+N-1|k}]$ and

$\Delta\bar{\mathbf{u}}_k^* := [\Delta\mathbf{u}_{k|k}^*, \ldots, \Delta\mathbf{u}_{k+N-1|k}^*]$. The first column of the optimal input trajectory $\Delta\bar{\mathbf{u}}_k^*$, denoted by $\Delta\mathbf{u}^*(k)$ or $\Delta\mathbf{u}_{k|k}^*$, is applied to the system combined with the current control law $\mathbf{u}(k)$. In other words, the feedback control law at time $k+1$ is $\mathbf{u}^*(k+1) := \mathbf{u}(k) + \Delta\mathbf{u}^*(k)$.

Remark 2: For this work, the cost function is defined in (17), to account for the incremental control signal $\Delta\mathbf{u}$ and do not consider the absolute control signal $\mathbf{u}$. Obviously, the cost function $J_N(\mathbf{X}(k), \Delta\bar{\mathbf{u}}(k), k)$ is a convex function because of its quadratic form. Besides, (17b) is an affine system and $\bar{\mathbb{X}}$ and $\mathbb{U}$ are convex sets. Therefore, OCP (18) is a convex optimization problem, and a unique optimal solution exists for nonempty admissible sets.

Remark 3: In existing MPC without terminal ingredients, comparing [17] and [18], the prediction is based on a nominal model. This requires to first identify the nominal model of the plant with high precision, whereas the proposed IMPC approach employs the incremental model based on TDE and, thus, it is not necessary to identify the model of $\mathbf{f}(\mathbf{x})$ and $\mathbf{g}(\mathbf{x})$ in (2b). Accordingly, the predictions are generated by the discrete-time linear system (13), where only $\bar{\mathbf{g}}$ is associated with the system model because $\bar{\mathbf{g}}$ is selected such that $\|\mathbf{I} - \mathbf{g}(\mathbf{x})\bar{\mathbf{g}}^{-1}\| < 1$. As stated in Remark 1, the sufficient condition for $\|\mathbf{I} - \mathbf{g}(\mathbf{x})\bar{\mathbf{g}}^{-1}\| < 1$ can be fulfilled by a large positive $\bar{g}_i$ even though the exact expression of $\mathbf{g}(\mathbf{x})$ is unknown.

IV. ISS Analysis

In Section III, the IMPC is developed without the concrete mathematical model, where the approximated discrete-time linear system (13) is used to generate predictions. However, the TDE error is inevitable and stability will be affected by this error. Stability will be investigated in the ISS framework and it is shown that for a large enough horizon, a bounded TDE error will allow that the reference trajectory is stabilized but not asymptotically reached. In this section, a definition of the reachable reference trajectory is first given. Then, some preliminary results are introduced, such as a local upper bound of the value function, an upper bound of the TDE error, and local continuity of the value function. Finally, the ISS of the proposed IMPC in local regions around reachable reference trajectories is investigated.

A. Reachable Reference Trajectory

In this section, a locally optimal incremental controller is developed for the discrete-time linear system (13), which is used to define the reachable reference trajectory.

1) Locally Optimal Incremental Controller: Let $\mathbf{E}(k) := \mathbf{X}(k) - \mathbf{X}_{\text{ref}}(k)$ be the tracking error. Assuming that input and state constraints are not violated, a locally optimal incremental control signal $\Delta\mathbf{u}_{\text{OI}}(\mathbf{X}(k), \mathbf{X}_{\text{ref}}(k))$ is designed considering (17a) as the cost function

$$\Delta\mathbf{u}_{\text{OI}}(\mathbf{X}(k), \mathbf{X}_{\text{ref}}(k)) = \Delta\hat{\mathbf{u}}_{\text{ref}}(k) + \mathbf{K}_0\mathbf{E}(k) \tag{19}$$

where $\mathbf{K}_0 = -(\mathbf{R}+\mathbf{B}^\top\mathbf{P}\mathbf{B})^{-1}\mathbf{B}^\top\mathbf{P}\mathbf{A}$, and $\mathbf{P} \succ 0$ is the solution to the following Riccati equation:

$$\mathbf{P} = \mathbf{A}^\top\mathbf{P}\mathbf{A} - \mathbf{A}^\top\mathbf{P}\mathbf{B}(\mathbf{R} + \mathbf{B}^\top\mathbf{P}\mathbf{B})^{-1}\mathbf{B}^\top\mathbf{P}\mathbf{A} + \mathbf{Q}.$$

To study stability, $V(\mathbf{E}(k)) := \|\mathbf{E}(k)\|_{\mathbf{P}}^2$ is considered as the Lyapunov function. Then, the difference is

$$\begin{aligned}\Delta V(\mathbf{E}(k+1)) &= V(\mathbf{E}(k+1)) - V(\mathbf{E}(k)) \\ &= \|\mathbf{E}(k+1)\|_{\mathbf{P}}^2 - \|\mathbf{E}(k)\|_{\mathbf{P}}^2 \\ &= -\mathbf{E}^\top(k)\big(\mathbf{Q} + \tilde{\mathbf{R}}\big)\mathbf{E}(k) \le 0\end{aligned} \tag{20}$$

where $\tilde{\mathbf{R}} := \mathbf{A}^\top\mathbf{P}\mathbf{B}(\mathbf{R}+\mathbf{B}^\top\mathbf{P}\mathbf{B})^{-1}\mathbf{R}(\mathbf{R}+\mathbf{B}^\top\mathbf{P}\mathbf{B})^{-1}\mathbf{B}^\top\mathbf{P}\mathbf{A}$ and $\tilde{\mathbf{R}} \succ 0$.

2) Definition of Reachable Reference Trajectory: Based on the locally optimal incremental controller, the definition of the reachable reference trajectory is introduced.

Definition 1: A reference trajectory $(\mathbf{X}_{\text{ref}}, \Delta\hat{\mathbf{u}}_{\text{ref}})$ is reachable if $\mathbf{X}_{\text{ref}}(k+i) \in \bar{\mathbb{X}}$ and $\|\mathbf{E}_{k+i|k}\|_{\mathbf{Q}}^2 \le c$ implies that $\mathbf{u}(k) \in \mathbb{U}$, $\mathbf{X}_{k+i|k} \in \bar{\mathbb{X}}$

$$\mathbf{u}_{\text{ref}}(k), \mathbf{u}_{\text{ref}}(k+i+1) := \mathbf{u}(k) + \sum_{m=0}^{i} \Delta\hat{\mathbf{u}}_{\text{ref}}(k+m) \in \mathbb{U}_{\text{ref}}$$

$$\mathbf{u}_{k+i+1|k} = \left(\mathbf{u}(k) + \sum_{m=0}^{i} \Delta\mathbf{u}_{\text{OI}}(\mathbf{X}_{k+m|k}, \mathbf{X}_{\text{ref}}(k+m))\right) \in \mathbb{U}$$

for $i \in \mathbb{I}_{[0,N-1]}$, $\mathbb{U}_{\text{ref}} \bigoplus \mathbb{C}_s \subseteq \mathbb{U}$ and $\mathbb{C}_s \subseteq \mathbb{R}^n := \{\mathbf{c} \in \mathbb{R}^n : -s\mathbf{1} \le \mathbf{c} \le s\mathbf{1}\}$, where $c, s \in \mathbb{R}_{\ge 0}$ are positive scalars and $\bigoplus$ denotes the Minkowski sum; otherwise, it is unreachable.

Similar to the definition of the reachable reference trajectory in [18], Definition 1 also requires that the trajectory can be tracked and lies strictly in the tightened constraint sets. However, it is not guaranteed that such a reachable reference trajectory still exists when the incremental control structure is adopted. Assuming that $\bar{\mathbf{g}}$ is selected such that $\|\mathbf{I} - \mathbf{g}(\mathbf{x})\bar{\mathbf{g}}^{-1}\| \le \delta < 1$, Lemma 1 is given, which verifies that the reachable reference trajectory exists and provides sufficient conditions of reachable reference trajectories.

Lemma 1: Suppose that there exists $c_x \in \mathbb{R}_{>0}$ such that $\|\mathbf{X}^i - \mathbf{X}_{\text{ref}}(k+i)\|_{\mathbf{Q}}^2 \le c_x$ $(i \in \mathbb{I}_{[0,N-1]})$ implies $\mathbf{X}^i \in \bar{\mathbb{X}}$. If the reference trajectory satisfies $\mu_2\big(k_1 r_{b1} + f_{\max} r_{b2} + \omega_{2,\max} + f_0\big) < \tau_{\max}$, $\big(f_{\max} r_{b2} + \bar{\bar{r}} + \omega_{2,\max} + f_0\big)/\bar{g}_{\min} < (1-\delta)\tau_{\max}$, and $\|\mathbf{E}(k)\|_{\mathbf{Q}}^2 \le c$, then, for $i \in \mathbb{I}_{[0,N-1]}$, $\mathbf{u}(k) \in \mathbb{U}$, $\mathbf{X}_{k+i|k} \in \bar{\mathbb{X}}$

$$\mathbf{u}_{\text{ref}}(k), \mathbf{u}_{\text{ref}}(k+i+1) := \mathbf{u}(k) + \sum_{m=0}^{i} \Delta\hat{\mathbf{u}}_{\text{ref}}(k+m) \in \mathbb{U}_{\text{ref}}$$

$$\mathbf{u}_{k+i+1|k} = \left(\mathbf{u}(k) + \sum_{m=0}^{i} \Delta\mathbf{u}_{\text{OI}}\big(\mathbf{X}_{k+m|k}, \mathbf{X}_{\text{ref}}(k+m)\big)\right) \in \mathbb{U}$$

and $\mathbb{U}_{\text{ref}} \bigoplus \mathbb{C}_s \subseteq \mathbb{U}$, where $c := \min\{c_u, (c_x/\tilde{\lambda})\}$, $s := \min\{s_1, s_2\}$, $c_u := \min\{c_1, c_2\}$, $\tilde{\lambda} := (\lambda_{\max}(\mathbf{Q})\lambda_{\max}(\mathbf{P})/\lambda_{\min}(\mathbf{Q})\lambda_{\min}(\mathbf{P}))$, $k_1 := \|\mathbf{K}_1\|$, $\mathbf{K}_1 := (1/T_s)[\mathbf{O}, \mathbf{I}, \mathbf{O}, -\mathbf{I}]$, $r_{b1} := 2\sqrt{(\bar{r}^2 + \bar{\bar{r}}^2)}$, $r_{b2} := \sqrt{2(\bar{r}^2 + \bar{\bar{r}}^2)}$, $\omega_{2,\max} := \max_{k\in\mathbb{I}_{>0}}\|\boldsymbol{\omega}_2(k)\|$, $\tau_{\max} := \min_{i\in\mathbb{I}_{[1,n]}}\tau_{i,\max}$, and $\bar{g}_{\min} := \lambda_{\min}(\bar{\mathbf{g}})$.

Note that s_1, c_1, s_2, and c_2 are given in (48), (49), (61), and (62), respectively.

Proof: Through exploring the working mechanism of the locally optimal incremental controller in the horizon, it is verified that reachable reference trajectories satisfying Definition 1 exist. For details, see Appendix A. ∎

Note that Lemma 1 is introduced to show existence of the reachable reference trajectory. Zooming techniques are used to derive the sufficient conditions of the reachable reference trajectory and it results in conservative results. In other words, even though the sufficient conditions are not satisfied, often some reference trajectories are nevertheless reachable. Moreover, the sufficient conditions in Lemma 1 are not related to the prediction horizon N. Hence, if the assumption ($\exists c_x \in \mathbb{R}_{>0}$ such that $\|\mathbf{X}^i - \mathbf{X}_{\text{ref}}(k+i)\| \leq c_x$ implies $\mathbf{X}^i \in \bar{\mathbb{X}}$) holds regardless of N, then Lemma 1 still holds when a large N is selected. In addition, it is not required to determine or construct reachable reference trajectories when the IMPC is implemented in practice. No matter for reachable or unreachable reference trajectory, the controller is obtained through solving the constrained OCP (18). The introduction of the reachable reference trajectory is merely a basis for local ISS analysis.

B. Preliminary Results

In this section, some preliminary results to analyze the ISS of IMPC are developed. Considering the locally optimal incremental controller (19) as the auxiliary control law, a local upper bound of the value function $V_N(\mathbf{X}(k), k)$ is derived for a reachable reference trajectory. Then, an upper bound of the TDE error is determined. Finally, the continuity of $V_N(\mathbf{X}(k), k)$ is proposed, which is used to avoid an overconservative cumulative error bound during the ISS analysis.

1) Local Upper Bound of Value Function: Considering a reachable reference trajectory, a local upper bound of $V_N(\mathbf{X}(k),k)$ is determined in Lemma 2.

Lemma 2: For a small enough tracking error $\|\mathbf{E}(k)\|_{\mathbf{Q}}^2 \leq c$, there exists $\kappa \in \mathbb{R}_{>0}$ such that $V_N(\mathbf{X}(k), k)$ is bounded by

$$V_N(\mathbf{X}(k), k) \leq \kappa \|\mathbf{E}(k)\|_{\mathbf{Q}}^2. \tag{21}$$

Proof: Given a reachable reference trajectory, a small enough tracking error $\|\mathbf{E}(k)\|_{\mathbf{Q}}^2 \leq c$ will allow to apply the locally optimal incremental controller (19) without violation of input or state constraints. Besides, due to optimality principle, $V_N(\mathbf{X}(k), k) \leq J_N(\mathbf{X}(k), \bar{\mathbf{u}}(k), k)$. Thus, if it is shown that the cost function $J_N(\mathbf{X}(k), \bar{\mathbf{u}}(k), k)$ is bounded under the function of the locally optimal incremental controller, then boundedness of the value function $V_N(\mathbf{X}(k), k)$ is also found.

For the locally optimal incremental controller (19), upper bounds for the tracking errors are obtained (cf. (58) in Appendix A), and for the control signals in the prediction horizon

$$\begin{aligned} \|\tilde{\Delta}\mathbf{u}_{k+i|k}\|_{\mathbf{R}}^2 &= \|\Delta\mathbf{u}_{\text{OI}}(\mathbf{X}_{k+i|k}, \mathbf{X}_{\text{ref}}(k+i)) - \Delta\mathbf{u}_{\text{ref}}(k+i)\|_{\mathbf{R}}^2 \\ &\leq K_{\max}\|\mathbf{E}_{k+i|k}\|_{\mathbf{Q}}^2 \end{aligned} \tag{22}$$

where $i \in \mathbb{I}_{[0,N-1]}$ and $K_{\max} := (\lambda_{\max}(\mathbf{R})\|\mathbf{K}_0\|_{\mathbf{R}}^2/\lambda_{\min}(\mathbf{Q}))$.

Thus, one has

$$\begin{aligned} V_N(\mathbf{X}(k), k) &\leq J_N(\mathbf{X}(k), \Delta\bar{\mathbf{u}}(k), k) \\ &= \sum_{i=0}^{N-1}\left(\|\mathbf{E}_{k+i|k}\|_{\mathbf{Q}}^2 + \|\tilde{\Delta}\mathbf{u}_{k+i|k}\|_{\mathbf{R}}^2\right) \\ &\overset{0<\rho<1}{\leq} \kappa\|\mathbf{E}(k)\|_{\mathbf{Q}}^2 \end{aligned} \tag{23}$$

where $\kappa := ((1+K_{\max})\lambda_{\max}(\mathbf{Q})\lambda_{\max}(\mathbf{P})/(1-\rho)\lambda_{\min}(\mathbf{Q})\lambda_{\min}(\mathbf{P}))$. ■

2) Upper Bound of TDE Error: In the sequel, an upper bound for the difference between state predictions using the approximated nominal dynamics (13) and the real state trajectory that results from (12) is quantified. To determine this upper bound, an upper bound of TDE error is first determined.

In [36]–[40], [44], and [45], the TDE error is verified to be bounded if a TDE-based controller is employed. However, in our approach, the incremental controller $\Delta\mathbf{u}(k)$ is obtained by solving the constrained OCP (18), and an analytic expression for $\Delta\mathbf{u}(k)$ is not available. In Lemma 3, the local continuity of uncertain functions and the input constraint will be used to analyze the boundedness of the TDE error.

Lemma 3: There exists $\epsilon^* \in \mathbb{R}_{>0}$ such that $\|\boldsymbol{\epsilon}\| \leq \epsilon^*$ for a sufficiently small sampling period.

Proof: See Appendix B. ■

Remark 4: Note that ϵ^* derived in Lemma 3 is overestimated. $\mathbf{H}(\mathbf{x}, \dot{\mathbf{x}})_{t-L}$ is used to approximate $\mathbf{H}(\mathbf{x}, \dot{\mathbf{x}})$ and L is usually selected as the sampling period. In practice, a digital control system can be regarded as a continuous system when the sampling rate is faster than 30 times the system bandwidth [51]. Thus, the smaller the sampling period, the smaller is the TDE error. In other words, for any choice of $\bar{\epsilon}^*$, a sufficiently small sampling period can be chosen such that $\|\boldsymbol{\epsilon}\| \leq \bar{\epsilon}^*$.

Thus, using (12) and (13) and Lemma 3, one obtains that

$$\|\mathbf{X}(k+1) - \mathbf{X}_{k+1|k}^*\| \leq \|\bar{\boldsymbol{\epsilon}}_2\| \leq \bar{\epsilon}^* \tag{24}$$

where $\bar{\epsilon}^* := \sqrt{2\left(\omega_{1,\max}^2 + \left(\bar{g}_{\max}\epsilon^* + 2\omega_{2,\max}\right)^2\right)T_s}$ and $\omega_{1,\max} := \max_{k\in\mathbb{I}_{\geq 0}}\|\boldsymbol{\omega}_1(k)\|$.

3) Continuity of Value Function: In the following, continuity property of the value function will be verified, based on local controllability of the system (13). At first, a set $\mathbb{D}$ ($\mathbb{D} \subseteq \bar{\mathbb{X}}$) will be introduced in Lemma 4, to show that if $\mathbf{X} \in \mathbb{D}$, then the optimal solutions lie strictly in the tightened constraint sets.

Lemma 4: There exist constants $V_{\max}$, $\tilde{s}$, $\tilde{r}_1 \in \mathbb{R}_{>0}$ such that optimal solutions starting from $\mathbf{X}$ ($\mathbf{X} \in \mathbb{D}$, $\mathbb{D} := \{\mathbf{X} \in \bar{\mathbb{X}} : V_N(\mathbf{X}, k) \leq V_{\max}\}$) satisfy tightened constraints, i.e., $\mathbf{X}_{k+i|k}^* \in \bar{\mathbb{X}}'$ and $\mathbf{u}_{k+i|k}^* \in \mathbb{U}'$ for all $i \in \mathbb{I}_{[0,N-1]}$, where $\bar{\mathbb{X}}' \bigoplus \mathbb{B}_{\tilde{r}_1} \subseteq \bar{\mathbb{X}}$ and $\mathbb{U}' \bigoplus \mathbb{C}_{\tilde{s}} \subseteq \mathbb{U}$.

Proof: First, it is verified that the reachable reference trajectory lies in the tightened constraint sets. According to the definition of the reachable reference trajectory (Definition 1), $\|\mathbf{E}_{k+i|k}\|_{\mathbf{Q}}^2 \leq c$ implies $\mathbf{X}_{k+i|k} \in \bar{\mathbb{X}}$ for all $i \in \mathbb{I}_{[0,N-1]}$. Thus, $\mathbf{X}_{\text{ref}}(k+i) \in \mathbb{X}_{\text{ref}}$ and $\mathbb{X}_{\text{ref}} \bigoplus \mathbb{B}_{\tilde{r}} \subseteq \bar{\mathbb{X}}$, where $\mathbb{B}_{\tilde{r}} \subseteq \mathbb{R}^{4n} := \{\mathbf{b} \in \mathbb{R}^{4n} : \|\mathbf{b}\| \leq \tilde{r}\}$ denotes a unitary ball with the radius $\tilde{r}$, and $\tilde{r} = \sqrt{(c/\lambda_{\max}(\mathbf{Q}))}$. Besides, $\mathbf{u}_{\text{ref}}(k+i) \in \mathbb{U}_{\text{ref}}$ and $\mathbb{U}_{\text{ref}} \bigoplus \mathbb{C}_s \subseteq \mathbb{U}$. Thus, the reachable reference trajectory lies strictly in the tightened constraint sets.

Then, the possibility that optimal solutions $\mathbf{X}_{k+i|k}^*$ and $\mathbf{u}_{k+i|k}^*$ also lie strictly in the tightened constraint sets is demonstrated using an extreme value. When $\|\mathbf{E}(k)\|_{\mathbf{Q}}^2 \leq \xi$ ($\xi \leq c$), the system is controllable. If ξ is sufficiently small, then the optimal solutions $\mathbf{X}_{k+i|k}^*$ and $\mathbf{u}_{k+i|k}^*$ converge and get close to the reference trajectory. Thus, it is reasonable to assume

that when $\|\mathbf{E}(k)\|_{\mathbf{Q}}^2 \leq \xi$, $\mathbf{X}_{k+i|k}^*$ and $\mathbf{u}_{k+i|k}^*$ strictly lie in the tightened constraint sets, i.e., there exist $\tilde{s}$, $\tilde{r}_1 \in \mathbb{R}_{>0}$ such that $\mathbf{X}_{k+i|k}^* \in \bar{\mathbb{X}}'$ and $\mathbf{U}_{k+i|k}^* \in \mathbf{U}'$ where $\bar{\mathbb{X}}' \bigoplus \mathbb{B}_{\tilde{r}_1} \subseteq \bar{\mathbb{X}}$ and $\mathbb{U}' \bigoplus \mathbb{C}_{\tilde{s}} \subseteq \mathbb{U}$.

In addition, when $\|\mathbf{E}(k)\|_{\mathbf{Q}}^2 \leq c$, $V_N(\mathbf{X}(k), k)$ is a decrescent function, i.e., $\|\mathbf{E}(k)\|_{\mathbf{Q}}^2 \leq V_N(\mathbf{X}(k), k) \leq \kappa \|\mathbf{E}(k)\|_{\mathbf{Q}}^2$ (cf. *Lemma 2*). Thus, $V_N(\mathbf{X}(k), k) \leq \xi$ guarantees that $\|\mathbf{E}(k)\|_{\mathbf{Q}}^2 \leq \xi$. Therefore, $V_{\max} \in \mathbb{R}_{>0}$ exists. ∎

Lemma 4 implies that if $\mathbf{X} \in \mathbb{D}$, then the optimal solutions lie strictly in the tightened constraint sets. Besides, the trajectory constituted by the optimal solutions starting from $\mathbf{X}$ can be tracked. Thus, the optimal solutions starting from $\mathbf{X}$ ($\mathbf{X} \in \mathbb{D}$), can be regarded as a reachable reference trajectory. If the initial error between $\mathbf{X}$ and $\mathbf{Y}$ is sufficiently small, then predictions starting from $\mathbf{Y}$ generated by the locally optimal incremental controller lie in feasible sets, in accordance with Definition 1. Thus, it is reasonable to make the following assumption.

Assumption 3: For $\mathbf{X} \in \mathbb{D}$ and $\mathbf{Y} \in \mathbb{R}^{4n}$, $\|\mathbf{Y} - \mathbf{X}\|_{\mathbf{Q}}^2 \leq c_d$ ($c_d \in \mathbb{R}_{>0}$) implies that $\forall i \in [0, N-1]$, $\mathbf{Y}_{k+i|k} \in \bar{\mathbb{X}}$ and $\mathbf{u}_{k+i|k}^{\mathbf{Y}} \in \mathbb{U}$, where $\mathbf{Y}_{k+i|k}$ and $\mathbf{u}_{k+i|k}^{\mathbf{Y}}$ are predictions generated by the locally optimal incremental controller $\Delta\mathbf{u}(\mathbf{Y}_{k+i}, \mathbf{X}_{k+i|k}^*)$

$$\Delta\mathbf{u}(\mathbf{Y}_{k+i}, \mathbf{X}_{k+i|k}^*) = \Delta\mathbf{u}_{\mathbf{X},k+i|k}^* + \mathbf{K}_0(\mathbf{Y}_{k+i} - \mathbf{X}_{k+i|k}^*) \quad (25)$$

where $\Delta\mathbf{u}_{\mathbf{X},k+i|k}^*$ is the optimal control signal corresponding to $\mathbf{X}$.

Based on Lemma 4 and Assumption 3, Lemma 5, about continuity of value function, is proposed, which will be used to determine the cumulative error bound when ISS is analyzed.

Lemma 5 (Continuity of Value Function): If $\mathbf{X} \in \mathbb{D}$, $\mathbf{Y} \in \bar{\mathbb{X}}$, and $\|\mathbf{X} - \mathbf{Y}\|_{\mathbf{Q}}^2 \leq c_d$, then

$$V_N(\mathbf{Y}, k) - V_N(\mathbf{X}, k) \leq \frac{K_\ell(1 + \|\mathbf{K}_0\|_{\mathbf{P}})}{1 - \sqrt{\rho}} \sqrt{\frac{\lambda_{\max}(\mathbf{P})}{\lambda_{\min}(\mathbf{Q})} c_d} \quad (26)$$

with a constant $K_\ell \in \mathbb{R}_{>0}$.

Proof: Since the stage cost (15) is quadratic, one obtains the following Lipschitz property of the stage cost function with a constant $K_\ell \in \mathbb{R}_{>0}$:

$$\begin{aligned} &|\ell(\mathbf{X}_{k+i|k}, \Delta\mathbf{u}_{\mathbf{X},k+i|k}, k+i) - \ell(\mathbf{Y}_{k+i|k}, \Delta\mathbf{u}_{\mathbf{Y},k+i|k}, k+i)| \\ &\quad \leq K_\ell\big(\|\mathbf{X}_{k+i|k} - \mathbf{Y}_{k+i|k}\|_{\mathbf{P}} + \|\Delta\mathbf{u}_{\mathbf{X},k+i|k} - \Delta\mathbf{u}_{\mathbf{Y},k+i|k}\|_{\mathbf{P}}\big) \end{aligned} \quad (27)$$

where $\Delta\mathbf{u}_{\mathbf{X},k+i|k}$ and $\Delta\mathbf{u}_{\mathbf{Y},k+i|k}$ are predicted control signals corresponding to $\mathbf{X}$ and $\mathbf{Y}$, respectively.

Considering that $\mathbf{X}_{k+i|k}^*$ and $\Delta\mathbf{u}_{\mathbf{X},k+i|k}^*$ are the optimal solutions starting from $\mathbf{X}$ and the fact that $\|\mathbf{X} - \mathbf{Y}\|_{\mathbf{Q}}^2 \leq c_d$, it is concluded that if the locally optimal incremental controller designed in (25) is employed, the generated predicted variables corresponding to $\mathbf{Y}$ will not violate constraints, according to *Assumption 3*. Thus, the following upper bound of the difference between $V_N(\mathbf{Y}, k)$ and $V_N(\mathbf{X}, k)$ is derived, employing $\Delta\mathbf{u}(\mathbf{Y}_{k+i}, \mathbf{X}_{k+i|k}^*)$ (25) as the auxiliary control law:

$$\begin{aligned} &V_N(\mathbf{Y}, k) - V_N(\mathbf{X}, k) \\ &\leq \quad J_N\big(\mathbf{Y}, \Delta\mathbf{u}_{\mathrm{OI}}(\mathbf{Y}_{k+i}, \mathbf{X}_{k+i|k}^*)\big) - V_N(\mathbf{X}, k) \\ &\leq \quad K_\ell \sum_{i=0}^{N-1} \|\mathbf{Y}_{k+i|k} - \mathbf{X}_{k+i|k}^*\|_{\mathbf{P}} \\ &\quad + K_\ell \sum_{i=0}^{N-1} \|\Delta\boldsymbol{u}(\mathbf{Y}_{k+i}, \mathbf{X}_{k+i|k}^*) - \Delta\mathbf{u}_{\mathbf{X},k+i|k}^*\|_{\mathbf{P}} \\ &\overset{(25),(20)}{\leq} \quad K_\ell(1 + \|\mathbf{K}_0\|_{\mathbf{P}}) \sum_{i=0}^{N-1} (\sqrt{\rho})^i \|\mathbf{X} - \mathbf{Y}\|_{\mathbf{P}} \\ &\leq \quad \frac{K_\ell(1 + \|\mathbf{K}_0\|_{\mathbf{P}})}{1 - \sqrt{\rho}} \sqrt{\frac{\lambda_{\max}(\mathbf{P})}{\lambda_{\min}(\mathbf{Q})} c_d}. \end{aligned} \quad (28)$$

∎

From (28), it is concluded that if $\mathbf{X} \in \mathbb{D}$, $\mathbf{Y} \in \bar{\mathbb{X}}$, and $\|\mathbf{X} - \mathbf{Y}\|_{\mathbf{Q}}^2 \leq c_d$, then the difference between $V_N(\mathbf{Y}, k)$ and $V_N(\mathbf{X}, k)$ is upper bounded, regardless of N.

C. ISS of the Proposed IMPC

The concept of ISS has been widely used in the stability analysis of systems with bounded additive uncertainties [30], [31], [52]. Definitions and criteria for ISS that will be used later are referred to Appendix C.

Motivated by [34] and [35], the continuity of the value function will be employed to complete the ISS analysis. In contrast to ISS analyses in [30] and [31], feasible control sequences are not required in this article. The continuity of the value function has been proven in Section IV-B, which is also different from [34] and [35]. Our approach has the advantage that when the difference between states $\mathbf{X}$ and $\mathbf{Y}$ is sufficiently small (i.e., $\|\mathbf{X} - \mathbf{Y}\|_{\mathbf{Q}}^2 \leq c_d$), the estimated upper bound of the difference between $V_N(\mathbf{X}, k)$ and $V_N(\mathbf{Y}, k)$ does not increase with increasing N.

In Theorem 1, considering a reachable reference trajectory, ISS of the IMPC with respect to the TDE error is analyzed. Finally, ISS of IMPC is proven by showing that $V_N(\mathbf{X}(k), k)$ is an ISS Lyapunov function.

Theorem 1: Let Assumptions 1–3 hold and suppose that $\bar{\epsilon}^*$ satisfies

$$\bar{\epsilon}^* \leq \sqrt{\frac{c_d}{\lambda_{\max}(\mathbf{Q})}}, \quad (29)$$

$$\epsilon_N := \frac{K_\ell(1 + \|\mathbf{K}_0\|_{\mathbf{P}})}{1 - \sqrt{\rho}} \sqrt{\frac{\lambda_{\max}(\mathbf{P})\lambda_{\max}(\mathbf{Q})}{\lambda_{\min}(\mathbf{Q})}} \bar{\epsilon}^* \leq \alpha_V(V_{\max}). \quad (30)$$

Considering a reachable reference trajectory, there exists $N_1 \in \mathbb{I}_{>0}$, such that for all $N > N_1$, $V_N(\mathbf{X}(k), k)$ with the initial value $V_N(\mathbf{X}(k_0), k_0) \leq V_{\max}$ satisfies

$$\alpha_1(\|\mathbf{E}(k)\|) \leq V_N(\mathbf{X}(k), k) \leq \alpha_2(\|\mathbf{E}(k)\|) \quad (31)$$

$$V_N(\mathbf{X}(k+1), k+1) - V_N(\mathbf{X}(k), k) \leq -\alpha_N(\|\mathbf{E}(k)\|) + \epsilon_N \quad (32)$$

where $\alpha_V(\cdot) \in \mathcal{K}$ and $\alpha_N(\cdot) \in \mathcal{K}_\infty$, i.e., $V_N(\mathbf{X}(k), k)$ is an ISS Lyapunov function.

Proof: It consists of three parts. Assuming that $V_N(\mathbf{X}(k), k) \leq V_{\max}$, Part 1 confirms that $V_N(\mathbf{X}(k), k)$ is a decrescent function, and Part 2 confirms that $V_N(\mathbf{X}(k), k)$ is decreasing regionally. Finally, Part 3 demonstrates that, for a large enough prediction horizon N, $V_N(\mathbf{X}(k), k) \leq V_{\max}$ holds recursively.

Part 1: A lower bound for $V_N(\mathbf{X}(k),k)$ is straightforwardly obtained from

$$V_N(\mathbf{X}(k),k) \geq \|\mathbf{E}(k)\|_{\mathbf{Q}}^2 \geq \lambda_{\min}(\mathbf{Q})\|\mathbf{E}(k)\|^2. \quad (33)$$

Define $\gamma_{V_{\max}} \in \mathbb{R}_{>0} := \max\{\kappa, (V_{\max}/c)\}$. $V_N(\mathbf{X}(k),k)$ is upper bounded according to Lemma 2 and the definition of $\gamma_{V_{\max}}$

$$V_N(\mathbf{X}(k),k) \leq \gamma_{V_{\max}}\|\mathbf{E}(k)\|_{\mathbf{Q}}^2 \leq \gamma_{V_{\max}}\lambda_{\max}(\mathbf{Q})\|\mathbf{E}(k)\|^2. \quad (34)$$

Therefore, from (33) and (34), $V_N(\mathbf{X}(k),k)$ is a decrescent function, i.e., $V_N(\mathbf{X}(k),k)$ satisfies (31), which is the first criterion of ISS Lyapunov function in Definition 3 [compare (70)] with $\alpha_1(x) := \lambda_{\min}(\mathbf{Q})x^2$ and $\alpha_2(x) := \gamma_{V_{\max}}\lambda_{\max}(\mathbf{Q})x^2$.

Part 2: In this part, the regional decreasing property of $V_N(\mathbf{X}(k),k)$ is analyzed, i.e., the relationship between $V_N(\mathbf{X}(k+1),k+1)$ and $V_N(\mathbf{X}(k),k)$ is constructed. To be able to analyze stability similar to [17] and [18], the value function $V_N(\mathbf{X}^*_{k+1|k},k+1)$ is selected as an auxiliary value function, and the relationship between $V_N(\mathbf{X}^*_{k+1|k},k+1)$ and $V_N(\mathbf{X}(k),k)$ is investigated for a large enough N. To avoid an overconservative cumulative error bound, the continuity of the value function is used to upper bound the difference between $V_N(\mathbf{X}(k+1),k+1)$ and $V_N(\mathbf{X}^*_{k+1|k},k+1)$. Finally, the relationship between $V_N(\mathbf{X}(k+1),k+1)$ and $V_N(\mathbf{X}(k),k)$ is determined.

Following [17] and [18], the relation between $V_N(\mathbf{X}^*_{k+1|k},k+1)$ and $V_N(\mathbf{X}(k),k)$ is determined for a large enough prediction horizon N ($N \geq N_1$):

$$V_N(\mathbf{X}^*_{k+1|k},k+1) \leq V_N(\mathbf{X}(k),k) - \phi_N\lambda_{\min}(\mathbf{Q})\|\mathbf{E}(k)\|^2 \quad (35)$$

where $\phi_N := 1-((\kappa-1)^M/\kappa^{M-2})$, $M \in \mathbb{I}_{>0} \geq \lceil 2(\ln\kappa/\ln\kappa - \ln(\kappa-1))\rceil$, and $N_1 \in \mathbb{I}_{>0} := \lceil M + \gamma_{V_{\max}} - 1\rceil$.

Note that the basic idea of the proof of (35) can be summarized as follows. For a large enough N, there exists a constant $k_x \in \mathbb{I}_{[0,N-M]}$ such that $\ell(\mathbf{X}^*_{k+k_x|k}, \Delta\mathbf{u}^*_{k+k_x|k}, k+k_x) \leq c$. Then, based on the local upper bound of the value function established in Lemma 2 and the dynamic programming principle, (35) is obtained (for the detailed proof, see [17], [18]).

To construct the relation between $V(\mathbf{X}(k+1),k+1)$ and $V_N(\mathbf{X}^*_{k+1|k},k+1)$ using Lemma 5, Lemma 6 is introduced.

Lemma 6: Assuming that $\bar{\epsilon}^* \leq \sqrt{(c_d/\lambda_{\max}(\mathbf{Q}))}$, if $\mathbf{X}(k) \in \mathbb{D}$ and $N \geq N_1$, then $\mathbf{X}^*_{k+1|k} \in \mathbb{D}$ and $\mathbf{X}(k+1) \in \bar{\mathbb{X}}$.

Proof: First, $\mathbf{X}^*_{k+1|k} \in \mathbb{D}$ is verified. According to (35), if $N \geq N_1$, then $V_N(\mathbf{X}^*_{k+1|k},k+1) \leq V_N(\mathbf{X}(k),k)$.

Given that $\mathbf{X} \in \mathbb{D}$, i.e., $V_N(\mathbf{X}(k),k) \leq V_{\max}$, one obtains that $V_N(\mathbf{X}^*_{k+1|k},k+1) \leq V_N(\mathbf{X}(k),k) \leq V_{\max}$, which implies that $\mathbf{X}^*_{k+1|k} \in \mathbb{D}$.

Then, $\mathbf{X}(k+1) \in \bar{\mathbb{X}}$ is confirmed. According to the TDE error bound in Lemma 3, one has $\|\mathbf{X}(k+1) - \mathbf{X}^*_{k+1|k}\| \leq \bar{\epsilon}^*$ [cf. (24)]. Thus, $\|\mathbf{X}(k+1) - \mathbf{X}^*_{k+1|k}\|_{\mathbf{Q}}^2 \leq \lambda_{\max}(\mathbf{Q})(\bar{\epsilon}^*)^2$. Since $\bar{\epsilon}^* \leq \sqrt{(c_d/\lambda_{\max}(\mathbf{Q}))}$, one obtains $\|\mathbf{X}(k+1) - \mathbf{X}^*_{k+1|k}\|_{\mathbf{Q}}^2 \leq c_d$. Therefore, according to Assumption 3, $\mathbf{X}(k+1) \in \bar{\mathbb{X}}$ is obtained. ∎

In accordance with Lemmas 5 and 6, one has

$$V_N(\mathbf{X}(k+1),k+1) \leq V_N(\mathbf{X}^*_{k+1|k},k+1) + \epsilon_N. \quad (36)$$

Finally, the relation between $V_N(\mathbf{X}(k+1),k+1)$ and $V_N(\mathbf{X}(k),k)$ is confirmed. Substituting (35) into (36) yields (32)

$$V_N(\mathbf{X}(k+1),k+1) - V_N(\mathbf{X}(k),k) \leq -\alpha_N(\|\mathbf{E}(k)\|) + \epsilon_N$$

where $\alpha_N(\|\mathbf{E}(k)\|) := \phi_N\lambda_{\min}(\mathbf{Q})\|\mathbf{E}(k)\|^2$.

Thus, as shown in (32), $V_N(\mathbf{X}(k),k)$ satisfies the second criterion of ISS Lyapunov function in *Definition 3* [compare (71)] where $\alpha_3(x) := \phi_N\lambda_{\min}(\mathbf{Q})x^2$ and $\varphi(x) := (K_\ell(1+\|\mathbf{K}_0\|_{\mathbf{P}})/1-\sqrt{\rho})\sqrt{(\lambda_{\max}(\mathbf{P})\lambda_{\max}(\mathbf{Q})/\lambda_{\min}(\mathbf{Q}))}x$.

Therefore, $V_N(\mathbf{X}(k),k)$ is an ISS Lyapunov function.

Part 3: In this part, it will be verified that $V_N(\mathbf{X}(k),k) \leq V_{\max}$ holds recursively, for a large enough N.

From (31) and (32), one has

$$V_N(\mathbf{X}(k+1),k+1) - V_N(\mathbf{X}(k),k) \leq -\alpha_V(V_N(\mathbf{X}(k),k)) + \epsilon_N \quad (37)$$

where $\alpha_V(\cdot) := \alpha_N \circ {\alpha_r}^{-1}(\cdot)$ and $\alpha_r(x) := \lambda_{\max}(\mathbf{Q})x^2$ are $\mathcal{K}_\infty$ functions.

If $\mathbf{X}(k) \in \mathbb{D}$, then $V_N(\mathbf{X}(k),k) \leq V_{\max}$. Thus, combining with the above analysis and assumption, one has

$$\begin{aligned} V_N(\mathbf{X}(k+1),k+1) &\overset{(37)}{\leq} (\mathrm{id}-\alpha_V)(V_N(\mathbf{X}(k),k)) + \epsilon_N \\ &\overset{(30)}{\leq} (\mathrm{id}-\alpha_V)(V_{\max}) + \alpha_V(V_{\max}) \\ &\leq V_{\max} \end{aligned} \quad (38)$$

where id is the identity function, i.e., $\mathrm{id}(x) = x$, for all $x \in \mathbb{R}$. Thus, if $\mathbf{X}(k) \in \mathbb{D}$, then $\mathbf{X}(k+1) \in \mathbb{D}$. Using induction, it is shown that $V_N(\mathbf{X}(k+j),k+j) \leq V_{\max}$ for all $j \in \mathbb{I}_{>0}$. Thus, $\mathbb{D}$ is a positive invariant set. Therefore, $V_N(\mathbf{X}(k),k) \leq V_{\max}$ holds recursively.

According to (38), $V_N(\mathbf{X}(k),k) \leq V_{\max}$ holds recursively if $N > N_1$. Given that $V_N(\mathbf{X}(k_0),k_0) \leq V_{\max}$, $V_N(\mathbf{X}(k),k) \leq V_{\max}$ holds for all $k \in \mathbb{I}_{[k_0,\infty)}$.

In conclusion, it is demonstrated that for all $N > N_1$ and initial state $\mathbf{X}(k_0)$ with $V_N(\mathbf{X}(k_0),k_0) \leq V_{\max}$, the system is local ISS for a reachable reference trajectory. ∎

Remark 5: The ISS analysis is based on the assumptions (29) and (30) for the TDE error. If the combined TDE and discretization error $\bar{\epsilon}^*$ is sufficiently small, these assumptions can be satisfied. According to (24), the magnitude of $\bar{\epsilon}^*$ mainly depends on the upper bound of the TDE error ϵ^*. As stated in Remark 4, by reducing the sampling period, the TDE error can be regulated as small as necessary. It is consistent with simulations in Section V-C, which displays the influences of the sampling period on the stability of the closed-loop system.

Remark 6: Different from the cumulative error bound $\left(L_s(L_{\mathbf{f}}{}^{N-1} - 1/L_{\mathbf{f}} - 1) + L_t L_{\mathbf{f}}{}^{N-1}\right)d$ (where $L_{\mathbf{f}}$, L_s, and L_t are Lipschitz constants and d is the upper bound of the disturbance) derived in [30] and [31], the cumulative error bound in this article $\epsilon_N := (K_\ell(1+\|\mathbf{K}_0\|_{\mathbf{P}})/1-\sqrt{\rho})\sqrt{(\lambda_{\max}(\mathbf{P})\lambda_{\max}(\mathbf{Q})/\lambda_{\min}(\mathbf{Q}))}\bar{\epsilon}^*$ does not increase as N increases. Similar to our approach, the continuity property of the value function is also used to investigate the local ISS of the MPC method in [34] and [35]. Unfortunately, for $\mathbf{A}$ in (13), its eigenvalue $\lambda(\mathbf{A}) > 1$.

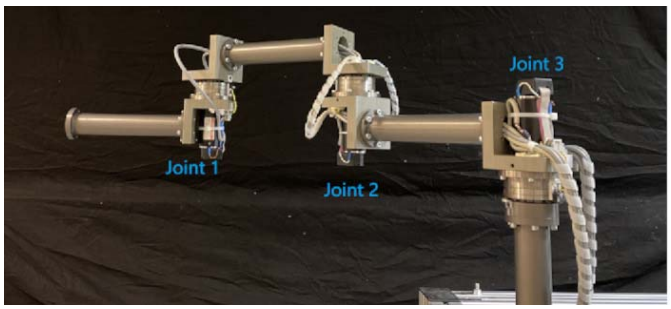

Fig. 1. Experimental setup of the 3-DoF robot manipulator.

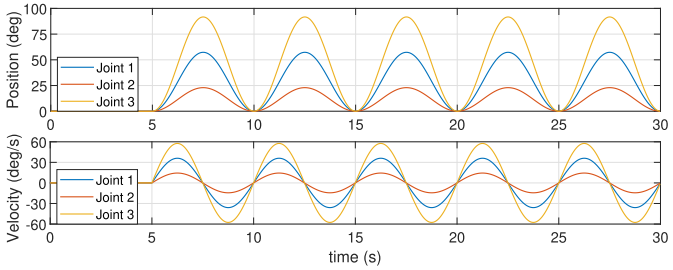

Fig. 2. Plots of reference trajectory for three joints.

It still results in the rise of the cumulative error bound with increasing N, if the method in [34] and [35] is applied.

Remark 7: Simply increasing the prediction horizon N can enlarge the region of attraction $\{\mathbf{X} \in \bar{\mathbb{X}} : V_N(\mathbf{X}, k) \leq V_{\max}\}$. This is because $N_1 := \lceil M + \gamma_{V_{\max}} - 1 \rceil$ increases as $\gamma_{V_{\max}} := (V_{\max}/c)$ increases. It is also verified by experiments in Section V.

Remark 8: According to Part 3, the system ultimately converges to $\mathbb{D}_t := \{\mathbf{X} \in \bar{\mathbb{X}} : V_N(\mathbf{X}, k) \leq \alpha_V^{-1}(\epsilon_N)\}$. Thus, $\|\mathbf{E}(k)\| \leq \sqrt{\alpha_V^{-1}(\epsilon_N)/\lambda_{\min}(\mathbf{Q})}$ according to (31). If we increase M (or N) properly, both $\alpha_N(\cdot)$ and $\alpha_V(\cdot)$ increase. Thus, the tracking error decreases if N increases properly. However, it does not asymptotically converge to zero because of the nonzero TDE error. The effects of N on the tracking errors are also investigated by experiments in Section V.

Remark 9: To guarantee ISS of IMPC in local regions around the reachable reference trajectory, the minimal prediction horizon $N_1 \in \mathbb{I}_{>0} := \lceil M + \gamma_{V_{\max}} - 1 \rceil$ is determined. Due to the zooming technique, this minimal N is very conservative (normally overestimated, compare [18]). However, a too large prediction horizon causes heavier computation such that the real-time control capability will be affected. Thus, a balance between ISS and computing efficiency has to be found in practice. To this end, based on current computing resources, the prediction horizon is selected as large as possible.

V. Experiment

In this section, the proposed IMPC is validated on a 3-DoF robot manipulator. First, to validate the optimal control performance of IMPC, comparison experiments with state-of-the-art TDE-based controllers are conducted. Then, to show capabilities to address input and state constraints, experiments are performed where step by step, the constraints are tightened. Finally, there is a discussion of the experimental results.

A. Experimental Setup

A custom-built 3-DoF robot manipulator is used throughout the experimental verification as shown in Fig. 1, where the order of the joint number is indicated. The mathematical model of the robot manipulator can be found in [53, Tables II–IV]. Nevertheless, note that the identified mathematical model is not used for the proposed IMPC. The manipulator is actuated by three torque-controlled motors (manufactured by Maxon) with a turn ratio of 1:100. Mounted on each motor, the incremental encoders offer the joint position measurement with a resolution of 2000. Using a peripheral component interconnect (PCI) communication card, the sensors and actuators are connected with the computer of which CPU is Intel Core i7-8086K @4.0 GHz. The executable algorithm is created by MATLAB 2017a in Ubuntu 14.04 LTS, using the first-order solver with a sampling rate of 1 kHz.

The parameters for IMPC are chosen as follows: diagonal matrix $\bar{\mathbf{g}} = \text{diag}(14, 32, 80)$, weighting matrices $\mathbf{Q} = \text{diag}\{500\mathbf{I}_3, 10\mathbf{I}_3, 50\mathbf{I}_3, \mathbf{I}_3\}$, and $\mathbf{R} = \text{diag}\{5, 5, 5\}$. Due to the TDE technique, the nonlinear system is approximated by a linear system (13), and then, the constrained OCP (18) is a quadratic-programming (QP) problem. Thus, the constrained OCP (18) is calculated by the active-set QP solver, qpOASES [54]. The prediction horizon $N = 15$ unless noted otherwise. Note that $\bar{\mathbf{g}}$ is selected by a manual tuning process, in practice. Generally, large $\bar{\mathbf{g}}$ results in large TDE errors, while small $\bar{\mathbf{g}}$ causes noisy responses. The constant $\bar{\mathbf{g}} := \text{diag}(\bar{g}_1, \ldots, \bar{g}_n)$ is selected following the procedures in [55] (the TDE parameter $\bar{\mathbf{g}}$ is corresponding to the inverse of $\bar{\mathbf{M}}$ in [55]): 1) start with a sufficiently large positive value for $\bar{g}_i$ to guarantee stability (compare Remark 1) and 2) decrease $\bar{g}_i$ until the closed-loop system almost shows a noisy response. Following the aforementioned procedures, the proposed IMPC is designed by tuning the TDE parameter $\bar{\mathbf{g}}$ without any information about the plant dynamics.

For the experimental study, six scenarios are considered. The reference trajectories for the three joints are chosen, as shown in Fig. 2. They are all sinusoidal reference trajectories. The period is 5 s and amplitudes are 28.65° (0.5 rad), 11.46° (0.2 rad), and 45.86° (0.8 rad). Then, reference velocity amplitudes are 36.11°/s (0.63 rad/s), 14.40°/s (0.25 rad/s), and 57.60°/s (1.01 rad/s).

Scenario 1 (Comparison With TDE-Based Controllers): To verify the optimal tracking performance of the proposed IMPC, it is compared to the time delay control (TDC[1]) [36] and TDC combined with SMC [40]. For simplicity, these controllers are referred to as IMPC, TDC, and TSMC. For IMPC, the input and state constraints are shown in Table I; For TDC and TSMC, the design parameters k_P and k_D are in general determined by the desired natural frequency ω_n and the damping ratio ζ, i.e., $k_P = \omega_n^2$ and $k_D = 2\zeta\omega_n$. Here, we set $\omega_n = 8$ rad/s and $\zeta = 1$. Thus, $k_P = 64$ and $k_D = 16$.

[1]TDC is a TDE-based controller, which is robust but not optimal.

TABLE I
INPUT AND STATE CONSTRAINTS OF SCENARIOS 1–5

Scenario No.	Angular constraint	Velocity constraint	Input constraint
1	114.59 deg	114.59 deg/s	4 N·m
2	114.59 deg	114.59 deg/s	2 N·m
3	63.03 deg	114.59 deg/s	4 N·m
4	114.59 deg	45.84 deg/s	4 N·m
5	63.03 deg	114.59 deg/s	2 N·m

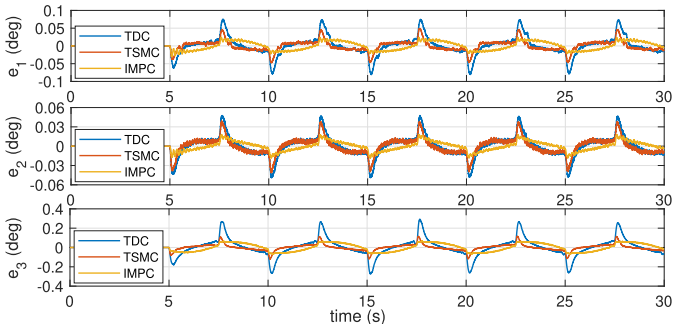

Fig. 3. Experimental results of Scenario 1: tracking errors for the three joints.

Besides, for TSMC, $\boldsymbol{\varepsilon} = [0.002, 0.001, 0.001]$, $\alpha = 50$, and $\varphi = 2.5 \times 10^4$, where $\boldsymbol{\varepsilon}$, α, and φ are all design parameters for the SMC. To quantify the tracking performance of these three controllers, the following average cost function is employed:

$$J = \frac{1}{N_t} \sum_{k=0}^{N_t} \left(\|\mathbf{E}(k)\|_{\mathbf{Q}}^2 + \|\tilde{\Delta}\mathbf{u}(k)\|_{\mathbf{R}}^2 \right) \tag{39}$$

where $N_t = t_s / T_s$, with t_s the terminal time.

Note that given the reference signals varying flatly lie strictly in the state set of Scenario 1, reference signals can be regarded as reachable reference trajectories in Scenario 1.

In Scenarios 2–5, the capability of IMPC to handle input and state constraints is verified, through tightening input and state constraints (see Table I). Note that $114.59^\circ = 2$ rad, $63.03^\circ = 1.1$ rad, and $45.84^\circ = 0.8$ rad.

In Scenario 6, Scenario 1 (only IMPC part) and Scenario 3 are repeated with $N = 8$, 12, and 15 to study the effect of different prediction horizons on tracking performance.

B. Experimental Results

The experimental results of Scenario 1 are shown in Figs. 3–5 and Table II. As shown in Fig. 3 and Table II, tracking errors of IMPC are smaller than those of TDC and TSMC. As shown in Fig. 4, especially the first subfigure, torque trajectories generated by IMPC are smoother than those of TDC and TSMC. This is because acceleration information, which is easily affected by measurement noise, is used to calculate torques directly for TDC and TSMC. For IMPC, the torques are generated by solving an OCP. The costs for the three controllers, calculated from (39), are 16.2475, 16.1185, and 3.3716. As expected, the cost for IMPC is much smaller than that of TDC and TSMC. Although tracking errors of

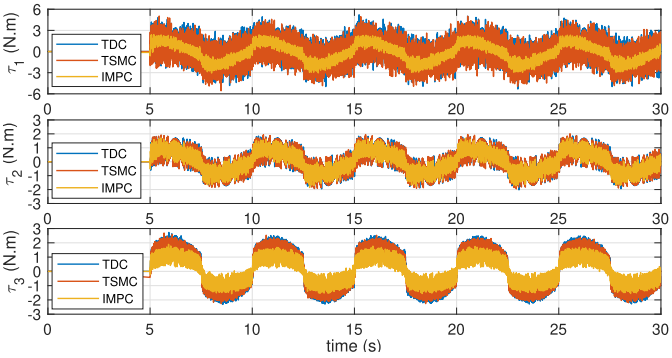

Fig. 4. Experimental results of Scenario 1: torques for three joints.

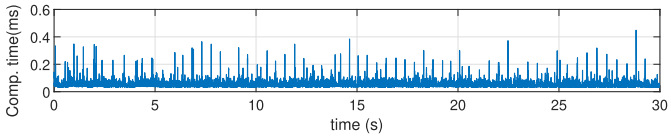

Fig. 5. Experimental results of Scenario 1: computing time.

TABLE II
EXPERIMENTAL RESULTS OF SCENARIO 1: RMS VALUES OF THE TRACKING ERRORS OF THE THREE JOINTS (10^{-2}deg)

Joint No.	TDC	TSMC	IMPC
1	2.38	1.36	1.17
2	1.50	1.16	0.68
3	8.56	3.05	3.93

TSMC are smaller than those of TDC, the related costs are almost equal. This is because nonsmooth torque trajectories result in large values for $\Delta\mathbf{u}$ and costs for TDC and TSMC mainly depend on variations of torque. As shown in Fig. 5, most of the computing time for each prediction horizon is smaller than 0.2 ms, which verifies real-time control capability.

The experimental results of Scenario 2 are shown in Fig. 6. As shown in Fig. 6, input constraints are not violated and the system is still stable, although the tracking errors are larger than that in Scenario 1.

The experimental results of Scenario 3 are shown in Fig. 7. It can be observed that the reference trajectory of joint 3 does sometimes leave the admissible set. Nevertheless, the closed-loop system is still stable. For the tracking errors, there are no apparent differences for joints 1 and 2, in comparison with Scenario 1. For joint 3, because of the strict state constraint, the tracking error is larger when reference signals are unreachable. It is also observed that during time intervals [8, 10] s, . . ., [28, 30] s, the tracking error of joint 3 gradually converges to a small neighborhood of the origin. There are two reasons for this phenomenon. One is that the reference trajectory is getting closer and finally approaches the feasible sets, and the other is that when the reference trajectory becomes reachable again, the tracking error ultimately converges to a small neighborhood around the origin. This coincides with the local ISS of the proposed IMPC analyzed in Section VI. For the torques of joint 3, there are severe variations for short

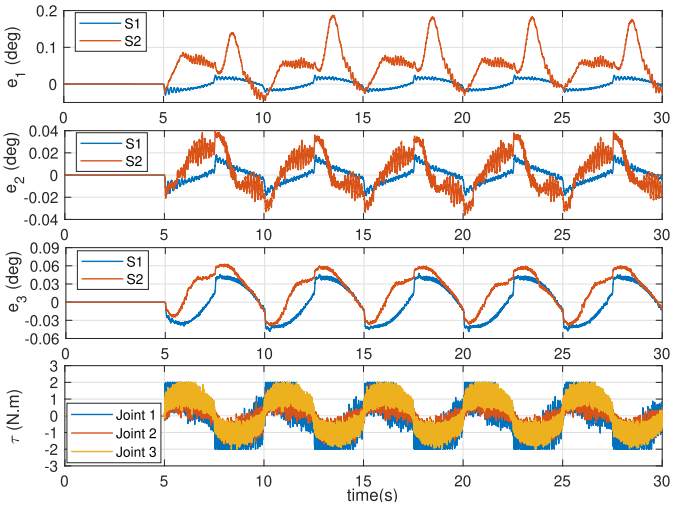

Fig. 6. Experimental results of Scenario 2: tracking errors and torques for three joints. Note that "S1" and "S2" represent variables generated in Scenarios 1 and 2, respectively.

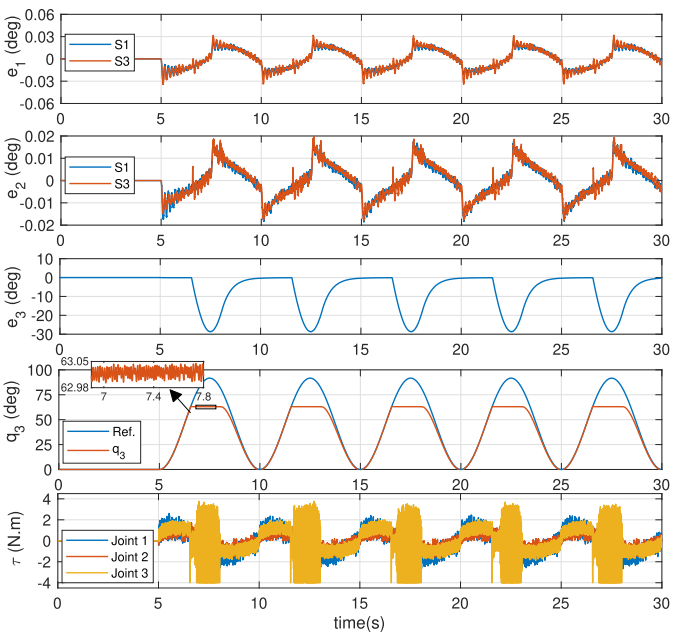

Fig. 7. Experimental results of Scenario 3: tracking errors, position of joint 3, and torques. Note that "S3" represent variables generated in Scenario 3.

periods when the positions are close to the boundary of the constraints. This is to avoid state constraint violation. On the other hand, joint 3 nearly stops moving, while joints 1 and 2 continue to move. The movement of joints 1 and 2 is regarded as the disturbance to joint 3. Despite severe variations, the whole closed-loop system is stable.

In Scenario 4, the state constraints are tightened for the angular velocity. The experimental results of Scenario 4 are shown in Fig. 8. For joints 1 and 2, there are no significant differences in tracking errors and tracking velocities between Scenarios 1 and 4. For joint 3, the velocity is limited because of the new constraint, resulting in a larger tracking error. As shown in the fifth subfigure of Fig. 8, the torque of joint 3 changes significantly during some time horizons, such as [6, 7] s, [8, 9] s, . . ., [28, 29] s. During these time horizons, the controller tries to avoid violation of the velocity constraints.

As shown in Figs. 7 and 8, especially the fourth subfigure of Fig. 7 and the fourth subfigure of Fig. 8, state constraints are slightly violated. This is because the TDE error and measurement noises are not considered when predictions are generated in the constrained OCP (18). Comparing Fig. 7 with Fig. 8, one learns that it is more difficult to constrain velocities because velocities are easily affected by measurement noise. Although the violation phenomenon occurs around the constraint boundary, the proposed IMPC scheme still has the capability to regulate states to a large extend.

The experimental results of Scenario 5 are shown in Fig. 9. In comparison with Scenario 1, the tracking error of joint 1 increases slightly because of the tightened input constraint. For joint 2, there are no significant differences. Joint 3 operates stably similar to Scenario 3.

The experimental results of Scenario 6 are shown in Figs. 10 and 11. For Scenario 1 with $N = 8$, 12, and 15, experimental results are shown in Fig. 10. The tracking error decreases for a longer horizon N. It coincides with the ISS analysis in Section IV-C. For $N = 12$ and 15, there are no significant differences in tracking errors. Due to the TDE

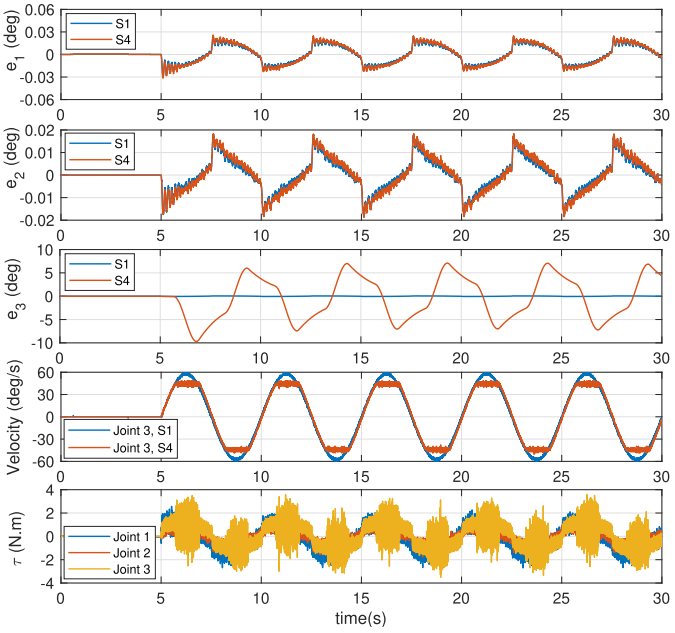

Fig. 8. Experimental results of Scenario 4: tracking errors, velocity of joint 3, and torques. Note that "S4" represent variables generated in Scenario 4.

error, the tracking error does not converge to zero even if N continues to increase.

The experimental results of Scenario 3 with different horizons are shown in Fig. 11. For joints 1 and 2, the reference is reachable and tracking errors decrease with increasing the horizon N. The reference trajectory for joint 3 is not always reachable. Although ISS for unreachable reference trajectories is not considered in the presented theory, system outputs stay close to reference signals. During the time intervals [8, 10] s, . . ., [28, 30] s, the unreachable reference trajectory switches

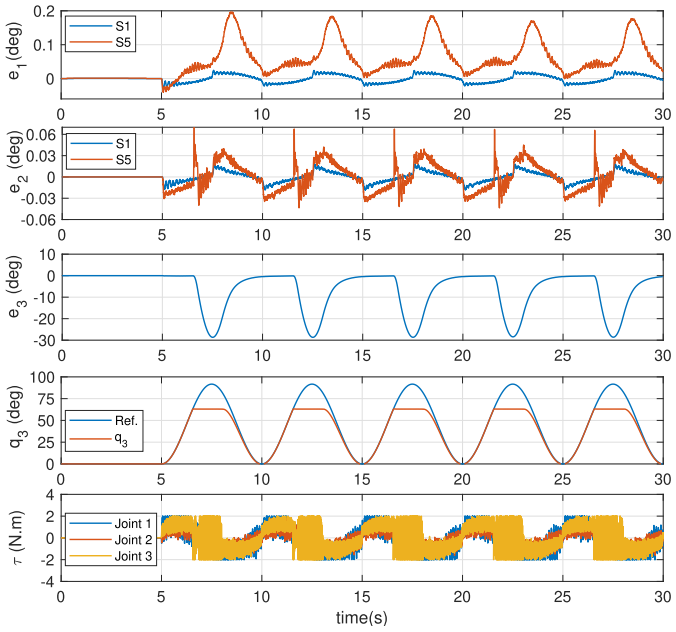

Fig. 9. Experimental results of Scenario 5: tracking errors, position of joint 3, and torques. Note that "S5" represent variables generated in Scenario 5.

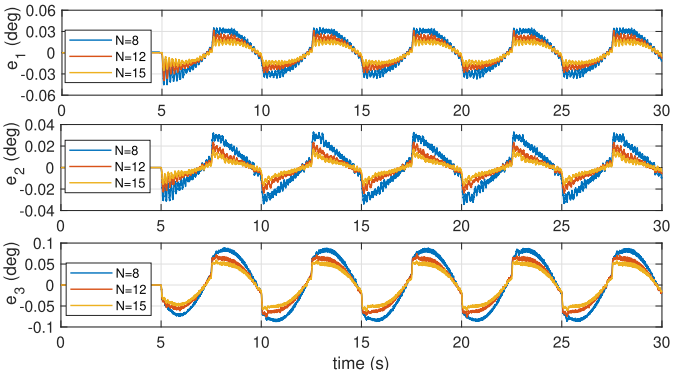

Fig. 10. Experimental results of Scenario 6: tracking errors with different prediction horizons.

to a reachable reference trajectory. As shown in Fig. 11, especially the fourth subfigure, as the horizon N increases, the output is closer to the reference signal. This is because the region of attraction increases and the tracking error decreases with larger N, as analyzed in Remarks 7 and 8.

C. Discussion

1) Prediction Horizon N: In Section IV, the minimal prediction horizon $N_1 := \lceil M + \gamma_{V_{\max}} - 1 \rceil$ can guarantee local ISS of IMPC for reachable reference tracking. Using the zooming technique, the method in Section IV to determine the prediction horizon N is very conservative. This phenomenon is illustrated using the following example. Assuming that $\|\mathbf{E}(k)\|_{\mathbf{Q}}^2 \leq c$, we obtain the theoretical minimal prediction horizon $N = 5.02\times10^{12}$. However, in Scenarios 1–6, yet, $N = 8$ allows for stability of the system. Thus, the minimal prediction horizon in ISS analysis is more of a conceptual nature.

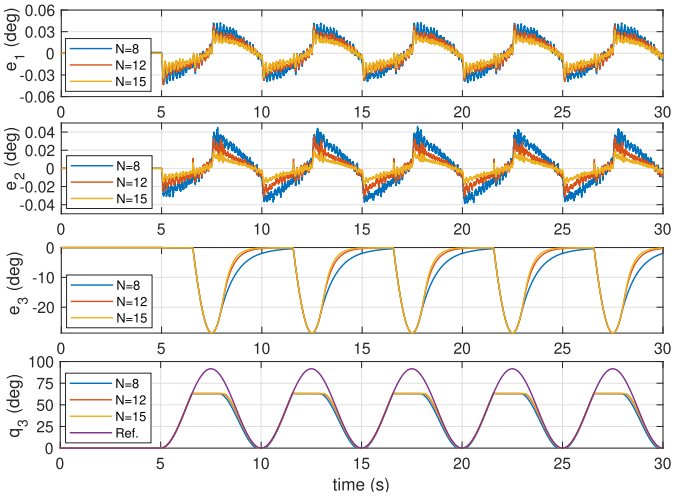

Fig. 11. Experimental results of Scenario 6: tracking errors and positions of joint 3 with different prediction horizons.

Besides, the statement in Remark 8 is verified by Scenario 6, i.e., tracking errors decrease with increasing the prediction horizon N. To this end, one would try to select a larger prediction horizon. On the other hand, increasing N causes heavier computation. Thus, in practice, one needs to find a compromise between tracking errors and computing efficiency. When the prediction horizon exceeds 15, real-time control cannot be realized sometimes because of the limited computational capability of our computer. As shown in Fig. 5, for reachable trajectories, there is still room to increase the prediction horizon. However, for unreachable trajectories, an iterative number of the qpOASES solver increases to keep constraints satisfaction, and it will also increase the computing time at the same time. Taking all factors discussed above into consideration, we find that for our application, $N = 15$ is a reasonable selection because it not only allows for real-time implementation but also guarantees precise enough tracking.

2) Reachable or Unreachable Reference Trajectory: During the implementation, one does not need to justify whether the reference trajectory is reachable or unreachable. We only need to solve the constrained OCP (18).

As shown in Lemma 1, if the set of admissible states is enlarged enough, an unreachable reference trajectory can be changed into a reachable reference trajectory. In other words, as shown in Scenarios 1–5, the reachable reference trajectory in Scenario 1 is changed into unreachable reference trajectories in Scenarios 2–4 after tighter input and/or state constraints are introduced. Although ISS of IMPC is not theoretically proven for unreachable reference trajectories, the reference trajectory is tracked as close as possible and the closed-loop system is still stable (as shown in Scenarios 2–5).

3) Limitations in Practice: To satisfy the assumptions with respect to the TDE error mentioned in Remark 5, a small enough sampling period is required. In our experiments, 0.001 s is used because of the setting of our experimental system, which is also commonly used in robotic systems, such as [9], [39]–[42], [45], and [53]. If the sampling period increases, the tracking error increases, and finally, the

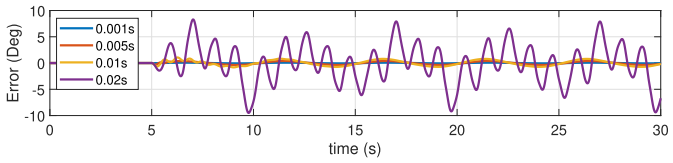

Fig. 12. Simulation results: tracking errors of Joint 1 with sampling periods $T_s = 0.001$, 0.005, 0.01, and 0.02 s.

closed-loop system becomes unstable. To check the influence of the sampling period on control performance and considering safety issues, simulations of Scenario 1 with different sampling periods ($T_s = 0.001$, 0.005, 0.01, and 0.02 s) are implemented. Because of space limitation, only tracking errors of joint 1 are displayed. As shown in Fig. 12, when $T_s = 0.001$, 0.005, and 0.01 s, tracking errors are very small. The tracking error increases as the sampling period increases since the TDE error increases with increasing the sampling period as analyzed in Section IV-B. For $T_s = 0.02$ s, the tracking error trajectory starts to oscillate because a larger TDE error affects solutions of the constrained OCP (18) and the system becomes unstable. Therefore, to receive reliable control performance, the sampling period should be smaller than 0.01 s. Besides, we need to consider real-time computation capability since the smaller sampling period, the heavier the burden of computing. In the experiment of this article, based on the simulation study, we select 0.001 s to ensure both the real-time computation and the tracking performance.

VI. Conclusion

In this article, an incremental model predictive controller for robot manipulators was proposed. Using TDE and discretization, an approximated discrete-time linear system with incremental control signal was derived. Based on the approximated discrete-time linear system, the IMPC was developed, and a mathematical model of the robot manipulator was no longer required. Employing local controllability of the system, the local ISS of IMPC was analyzed. To validate the proposed IMPC, a set of real-time experiments was performed. The results demonstrate the efficacy of the proposed IMPC in realizing optimal control performance while guaranteeing that input and state constraints are not violated, without concrete mathematical model of the robot manipulator.

Future research will be devoted to studying IMPC with strict constraints. The uncertain TDE error has to be addressed to guarantee strict state constraint satisfaction, and tube-based MPC [56] and data-driven and/or safe learning methods [57]–[59] are clues. As another future development, an optimal $\bar{\mathbf{g}}$ will be obtained online through an efficient learning algorithm with a properly minimized dataset.

Appendix A
Proof of Lemma 1

Proof: First, a sufficient condition for $\mathbf{u}(k) \in \mathbb{U}$ is derived. The state $\mathbf{x}(k) := \mathrm{col}(\mathbf{x}_1(k), \mathbf{x}_2(k))$ satisfies the following differential equation [see (2b)]:

$$\dot{\mathbf{x}}_2(k) = \mathbf{f}(\mathbf{x}(k)) + \mathbf{g}(\mathbf{x}(k))\mathbf{u}(k). \tag{40}$$

Discretizing $\dot{\mathbf{x}}_2(k)$ with the discretization error $\boldsymbol{\omega}_2(k)$ yields

$$\left(\mathbf{x}_{2,k|k} - \mathbf{x}_{2,k-1|k}\right)/T_s = \dot{\mathbf{x}}_2(k) + \boldsymbol{\omega}_2(k). \tag{41}$$

Replacing $\dot{\mathbf{x}}_2(k)$ in (40) by (41) yields

$$\mathbf{u}(k) = \mathbf{g}^{-1}(\mathbf{x}(k))\left[\left(\mathbf{x}_{2,k|k} - \mathbf{x}_{2,k-1|k}\right)/T_s - \boldsymbol{\omega}_2(k) - \mathbf{f}(\mathbf{x}(k))\right]. \tag{42}$$

According to Property 1 and Assumption 1, one has

$$\|\mathbf{u}(k)\| \le \mu_2\left(\|\mathbf{K}_1\mathbf{X}(k)\| + \omega_{2,\max} + f_{\max}\|\mathbf{x}(k)\| + f_0\right). \tag{43}$$

In accordance with Assumption 2, it is obtained that

$$\|\mathbf{K}_1\mathbf{X}(k)\| \le \|\mathbf{K}_1\|(\|\mathbf{E}(k)\| + \|\mathbf{X}_{\mathrm{ref}}(k)\|) \le k_1(\|\mathbf{E}(k)\| + r_{b1}) \tag{44}$$

$$\|\mathbf{x}(k)\| \le \|\mathbf{e}(k)\| + \|\mathbf{x}_{\mathrm{ref}}(k)\| \le \|\mathbf{E}(k)\| + r_{b2}. \tag{45}$$

Substituting (44) and (45) into (43) yields

$$\|\mathbf{u}(k)\| \le \mu_2\left((k_1 + f_{\max})\|\mathbf{E}(k)\| + k_1 r_{b1} + f_{\max} r_{b2} + \omega_{2,\max} + f_0\right). \tag{46}$$

In Section III-A, $|\tau_i| \le \tau_{i,\max}$ is specified. Thus, from (46), the following sufficient conditions are derived such that $\|\mathbf{u}(k)\| \le \tau_{\max}$ and $\|\mathbf{u}_{\mathrm{ref}}(k)\| \le \tau_{\max} - s$, i.e., $\mathbf{u}(k) \in \mathbb{U}$, $\mathbf{u}_{\mathrm{ref}}(k) \in \mathbb{U}_{\mathrm{ref}}$, and $\mathbb{U}_{\mathrm{ref}} \bigoplus \mathbb{C}_s \subseteq \mathbb{U}$

$$\mu_2\left(k_1 r_{b1} + f_{\max} r_{b2} + \omega_{2,\max} + f_0\right) < \tau_{\max} \tag{47}$$

$$s \le \underbrace{\tau_{\max} - \mu_2\left(k_1 r_{b1} + f_{\max} r_{b2} + \omega_{2,\max} + f_0\right)}_{s_1 \in \mathbb{R}_{>0}} \tag{48}$$

$$\|\mathbf{E}(k)\|_{\mathbf{Q}}^2 \le \underbrace{\lambda_{\min}(\mathbf{Q})\left(\frac{\tau_{\max} - \mu_2\left(k_1 r_{b1} + f_{\max} r_{b2} + \omega_{2,\max} + f_0\right)}{\mu_2(k_1 + f_{\max})}\right)^2}_{c_1 \in \mathbb{R}_{>0}}. \tag{49}$$

Second, incremental control signals and predicted states in the horizon are calculated by recursion.

Introducing $\bar{\mathbf{g}}$, $\mathbf{u}(k)$ is expressed as follows using (40):

$$\mathbf{u}(k) = \bar{\mathbf{g}}^{-1}[\dot{\mathbf{x}}_2(k) - \mathbf{f}(\mathbf{x}(k)) - (\mathbf{g}(\mathbf{x}(k)) - \bar{\mathbf{g}})\mathbf{u}(k)]. \tag{50}$$

Replacing $\dot{\mathbf{x}}_2(k)$ in (50) by (41) yields

$$\mathbf{u}(k) = \bar{\mathbf{g}}^{-1}\left[\left(\mathbf{x}_{2,k|k} - \mathbf{x}_{2,k-1|k}\right)/T_s - \boldsymbol{\omega}_2(k) - \mathbf{f}(\mathbf{x}(k))\right] - \bar{\mathbf{g}}^{-1}(\mathbf{g}(\mathbf{x}(k)) - \bar{\mathbf{g}})\mathbf{u}(k). \tag{51}$$

Recall $\Delta\mathbf{u}_{\mathrm{OI}}(\mathbf{X}(k), \mathbf{X}_{\mathrm{ref}}(k))$ in (19), (19) is rewritten as

$$\Delta\mathbf{u}_{\mathrm{OI}}(\mathbf{X}(k), \mathbf{X}_{\mathrm{ref}}(k)) = \bar{\mathbf{g}}^{-1}\left(\ddot{\mathbf{q}}_{\mathrm{ref}}(k+1) - \hat{\dot{\mathbf{x}}}_2(k) + \mathbf{K}_2\mathbf{E}(k)\right) \tag{52}$$

where $\hat{\dot{\mathbf{x}}}_2(k) := \left(\mathbf{x}_{2,k|k} - \mathbf{x}_{2,k-1|k}\right)/T_s$ is the approximated derivative and $\mathbf{K}_2 := \bar{\mathbf{g}}\mathbf{K}_0 + \mathbf{K}_1$. Thus, $\mathbf{u}_{k+1|k}$ is

$$\begin{aligned}\mathbf{u}_{k+1|k} &= \mathbf{u}(k) + \Delta\mathbf{u}_{\mathrm{OI}}(\mathbf{X}(k), \mathbf{X}_{\mathrm{ref}}(k)) \\ &= \bar{\mathbf{g}}^{-1}\left[-\mathbf{f}(\mathbf{x}(k)) + \mathbf{K}_2\mathbf{E}(k) + \ddot{\mathbf{q}}_{\mathrm{ref}}(k+1) - \boldsymbol{\omega}_2(k)\right] \\ &\quad - \bar{\mathbf{g}}^{-1}[\mathbf{g}(\mathbf{x}(k)) - \bar{\mathbf{g}}]\mathbf{u}(k).\end{aligned} \tag{53}$$

Applying $\Delta\mathbf{u}_{\mathrm{OI}}(\mathbf{X}(k), \mathbf{X}_{\mathrm{ref}}(k))$ to (13), $\dot{\mathbf{x}}_{2,k+1|k}$ is

$$\left(\mathbf{x}_{2,k+1|k} - \mathbf{x}_{2,k|k}\right)/T_s$$

$$= \big(\mathbf{x}_{2,k|k}-\mathbf{x}_{2,k-1|k}\big)/T_s+\bar{\mathbf{g}}\Delta\mathbf{u}_{\mathrm{OI}}(\mathbf{X}(k),\mathbf{X}_{\mathrm{ref}}(k))$$
$$\overset{(40),(41)}{=} \mathbf{f}(\mathbf{x}(k))+\bar{\mathbf{g}}\mathbf{u}_{k+1|k}+(\mathbf{g}(\mathbf{x}(k))-\bar{\mathbf{g}})\mathbf{u}(k)+\boldsymbol{\omega}_2(k). \quad (54)$$

From (54), $\mathbf{u}_{k+1|k}$ is expressed using $\mathbf{x}_{2,k+1|k}$ and $\mathbf{x}_{2,k|k}$

$$\mathbf{u}_{k+1|k} = \bar{\mathbf{g}}^{-1}\big[\big(\mathbf{x}_{2,k+1|k}-\mathbf{x}_{2,k|k}\big)/T_s-\boldsymbol{\omega}_2(k)-\mathbf{f}(\mathbf{x}(k))\big] - \bar{\mathbf{g}}^{-1}(\mathbf{g}(\mathbf{x}(k))-\bar{\mathbf{g}})\mathbf{u}(k). \quad (55)$$

Similarly, at time $k+i$, the predicted control signal is

$$\mathbf{u}_{k+i|k} = \bar{\mathbf{g}}^{-1}\big(-\mathbf{f}(\mathbf{x}(k))+\mathbf{K}_2\mathbf{E}_{k+i-1|k}+\ddot{\mathbf{q}}_{\mathrm{ref}}(k+i)-\boldsymbol{\omega}_2(k)\big) - \bar{\mathbf{g}}^{-1}(\mathbf{g}(\mathbf{x}(k))-\bar{\mathbf{g}})\mathbf{u}(k). \quad (56)$$

Finally, sufficient conditions for that input and state constraints in the horizon are not violated are determined.

As assumed, $\bar{\mathbf{g}}$ is selected such that $\|\mathbf{I}-\mathbf{g}(\mathbf{x})\bar{\mathbf{g}}^{-1}\| \le \delta < 1$. Besides, according to (20), the following inequalities are obtained:

$$\|\mathbf{E}_{k+i|k}\|^2 \le \bar{\lambda}\rho^{i-1}\|\mathbf{E}(k)\|^2 \quad (57)$$
$$\|\mathbf{E}_{k+i|k}\|_{\mathbf{Q}}^2 \le \tilde{\lambda}\rho^{i-1}\|\mathbf{E}(k)\|_{\mathbf{Q}}^2 \quad (58)$$

where $\bar{\lambda} := (\lambda_{\max}(\mathbf{P})/\lambda_{\min}(\mathbf{P}))$ and $\rho := 1-(\lambda_{\min}\big(\mathbf{Q}+\tilde{\mathbf{R}}\big)/\lambda_{\max}(\mathbf{P})) < 1$.

In accordance with Assumptions 1 and *2*, (45), (56), and (57), one has

$$\|\mathbf{u}_{k+i|k}\| \le \frac{\Big(f_{\max}+k_{\max}\sqrt{\bar{\lambda}}\Big)\|\mathbf{E}(k)\|+f_{\max}r_{b2}+\bar{\bar{r}}+\omega_{2,\max}+f_0}{\bar{g}_{\min}}+\delta\tau_{\max} \quad (59)$$

where $k_{\max} := \|\mathbf{K}_2\|$. According to (59), a sufficient condition for $\mathbf{u}_{k+i|k} \in \mathbb{U}$ and $\mathbf{u}_{\mathrm{ref}}(k+i) \in \mathbb{U}_{\mathrm{ref}}$ is obtained

$$\big(f_{\max}r_{b2}+\bar{\bar{r}}+\omega_{2,\max}+f_0\big)/\bar{g}_{\min} < (1-\delta)\tau_{\max} \quad (60)$$
$$s \le \underbrace{\tau_{\max}-\big(f_{\max}r_{b2}+\bar{\bar{r}}+\omega_{2,\max}+f_0\big)/(\bar{g}_{\min}(1-\delta))}_{s_2\in\mathbb{R}_{>0}} \quad (61)$$

$$\|\mathbf{E}(k)\|_{\mathbf{Q}}^2 \le \underbrace{\lambda_{\min}(\mathbf{Q})\left(\frac{(1-\delta)\bar{g}_{\min}\tau_{\max}-f_{\max}r_b-\bar{\bar{r}}-\omega_{2,\max}-f_0}{f_{\max}+k_{\max}\sqrt{\bar{\lambda}}}\right)^2}_{c_2\in\mathbb{R}_{>0}}. \quad (62)$$

From (47), (49), (60), and (62), it is concluded that if the reference trajectory satisfies (47) and (60) and $\|\mathbf{E}(k)\|_{\mathbf{Q}}^2 \le c_u$, then $\forall i \in \mathbb{I}_{[0,N]}$, $\mathbf{u}_{k+i|k} \in \mathbb{U}$ and $\mathbf{u}_{\mathrm{ref}}(k+i) \in \mathbb{U}_{\mathrm{ref}}$.

Besides, if $\|\mathbf{E}(k)\|_{\mathbf{Q}}^2 \le c_x/\lambda$, according to (58), then $\|\mathbf{E}_{k+i|k}\|_{\mathbf{Q}}^2 \le c_x$, $\forall i \in \mathbb{I}_{[0,N-1]}$, that is, $\mathbf{X}_{k+i|k} \in \bar{\mathbb{X}}$.

Therefore, if the reference trajectory satisfies (47) and (60), $\|\mathbf{E}(k)\|_{\mathbf{Q}}^2 \le c$ guarantees local controllability of (13). ■

APPENDIX B
PROOF OF LEMMA 3

Proof: According to (6) and (7), $\boldsymbol{\epsilon}$ is rewritten as

$$\boldsymbol{\epsilon} = \big(\bar{\mathbf{g}}^{-1}-\mathbf{g}^{-1}(\mathbf{x})\big)(\dot{\mathbf{x}}_2-\dot{\mathbf{x}}_{2,0})+\big(\mathbf{g}^{-1}(\mathbf{x}_0)-\mathbf{g}^{-1}(\mathbf{x})\big)\dot{\mathbf{x}}_{2,0} + \mathbf{g}^{-1}(\mathbf{x})\mathbf{f}(\mathbf{x})-\mathbf{g}^{-1}(\mathbf{x}_0)\mathbf{f}(\mathbf{x}_0). \quad (63)$$

Since $\dot{\mathbf{x}}_2 = \mathbf{f}(\mathbf{x})+\mathbf{g}(\mathbf{x})\mathbf{u}$, one has

$$\dot{\mathbf{x}}_2-\dot{\mathbf{x}}_{2,0} = \mathbf{f}(\mathbf{x})-\mathbf{f}(\mathbf{x}_0)+\mathbf{g}(\mathbf{x})\Delta\mathbf{u}+(\mathbf{g}(\mathbf{x})-\mathbf{g}(\mathbf{x}_0))\mathbf{u}_0. \quad (64)$$

Substituting (64) into (63) yields

$$\boldsymbol{\epsilon} = \big(\bar{\mathbf{g}}^{-1}\mathbf{g}(\mathbf{x})-\mathbf{I}\big)\Delta\mathbf{u}+\big(\bar{\mathbf{g}}^{-1}\mathbf{g}(\mathbf{x})-\mathbf{I}\big)\mathbf{g}^{-1}(\mathbf{x})\mathbf{r}_1+\mathbf{r}_2 \quad (65)$$

where $\mathbf{r}_1 := \mathbf{f}(\mathbf{x})-\mathbf{f}(\mathbf{x}_0)+(\mathbf{g}(\mathbf{x})-\mathbf{g}(\mathbf{x}_0))\ \mathbf{u}_0$ and $\mathbf{r}_2 := \big(\mathbf{g}^{-1}(\mathbf{x}_0)-\mathbf{g}^{-1}(\mathbf{x})\big)\dot{\mathbf{x}}_{2,0}+\mathbf{g}^{-1}(\mathbf{x})\mathbf{f}(\mathbf{x})-\mathbf{g}^{-1}(\mathbf{x}_0)\mathbf{f}(\mathbf{x}_0)$.

For a sufficiently small sampling period, $\mathbf{r}_1$ and $\mathbf{r}_2$ are all bounded, i.e., there exist r_1, $r_2 \in \mathbb{R}_{>0}$ such that $\|\mathbf{r}_1\| \le r_1$ and $\|\mathbf{r}_2\| \le r_2$ [45].

According to Property 1 and the fact that $\mathbf{g}^{-1}(\mathbf{x}) = \mathbf{M}(\mathbf{q})$, one obtains $\|\mathbf{g}^{-1}(\mathbf{x})\| \le \mu_2$. Moreover, as stated in Section II-B, $\bar{\mathbf{g}}$ is selected such that $\|\mathbf{I}-\mathbf{g}(\mathbf{x})\bar{\mathbf{g}}^{-1}\| \le \delta < 1$. Thus,

$$\begin{aligned}\|\boldsymbol{\epsilon}\| &\le \|\big(\bar{\mathbf{g}}^{-1}\mathbf{g}(\mathbf{x})-\mathbf{I}\big)\|\|\Delta\mathbf{u}\| \\ &\quad+\|\big(\bar{\mathbf{g}}^{-1}\mathbf{g}(\mathbf{x})-\mathbf{I}\big)\|\|\mathbf{g}^{-1}(\mathbf{x})\|\|\mathbf{r}_1\|+\|\mathbf{r}_2\| \\ &\le \delta\|\Delta\mathbf{u}\|+\delta\mu_2 r_1+r_2. \end{aligned} \quad (66)$$

For IMPC, $\Delta\mathbf{u}$ is obtained solving the constrained OCP (18) such that $\mathbf{u} \in \mathbb{U}$. As stated in Section III-A, $\|\mathbf{u}\| \le u_{\max}$. Thus, $\Delta u_{\max} := \max\|\Delta\mathbf{u}\| = \max\|\mathbf{u}-\mathbf{u}_0\| \le 2\,u_{\max}$. Therefore, the TDE error is bounded by

$$\|\boldsymbol{\epsilon}\| \le 2\delta u_{\max}+\delta\mu_2 r_1+r_2 := \epsilon^*. \quad (67)$$

■

APPENDIX C
DEFINITIONS AND CRITERIA FOR ISS

Definition 2 [30], [52]: Consider a system given by

$$\mathbf{x}(k+1) = \mathbf{F}(\mathbf{x}(k),\mathbf{w}(k)) \quad (68)$$

where $\mathbf{x}(k) \in \mathbb{R}^n$ and $\mathbf{w}(k) \in \mathbb{R}^m$ ($m \le n$) are the state and disturbance of the system (68), respectively. Besides, there exists a constant $\gamma \in \mathbb{R}_{>0}$ such that $\|\mathbf{w}(k)\| \le \gamma$ for all k. Then, the system (68) is input-to-state stable if there exist $\beta(\cdot,\cdot) \in \mathcal{KL}$ and $\eta(\cdot) \in \mathcal{K}$ such that

$$\|\mathbf{x}(k)\| \le \beta(\mathbf{x}(0),k)+\eta(\gamma) \quad (69)$$

where $\mathbf{x}(0)$ is the initial value.

Definition 3 [30], [52]: A continuous function $V(\cdot)$ is an ISS Lyapunov function for the system (68) if there exist functions $\alpha_1(\cdot)$, $\alpha_2(\cdot)$, $\alpha_3(\cdot) \in \mathcal{K}_\infty$ and $\varphi(\cdot) \in \mathcal{K}$ such that

$$\alpha_1(\|\mathbf{x}(k)\|) \le V(\mathbf{x}(k)) \le \alpha_2(\|\mathbf{x}(k)\|) \quad (70)$$
$$V(\mathbf{F}(\mathbf{x}(k),\mathbf{w}(k)))-V(\mathbf{x}(k)) \le -\alpha_3(\|\mathbf{x}(k)\|)+\varphi(\gamma) \quad (71)$$

where $\varphi(\gamma)$ is the cumulative error bound.

Proposition 1 [30], [52]: If the system (68) admits an ISS Lyapunov function, then it is ISS.

ACKNOWLEDGMENT

The authors would like to thank Prof. Lars Grüne from the University of Bayreuth for useful discussions and suggestions to improve the quality of this article. They would also like to thank our master students Yang Liu, Zeyue Yang, and Zhiyuan Ji for their help to do experiments.

REFERENCES

[1] K. Kaltsoukalas, S. Makris, and G. Chryssolouris, "On generating the motion of industrial robot manipulators," *Robot. Comput.-Integr. Manuf.*, vol. 32, pp. 65–71, Apr. 2015.

[2] Z. Ma and P. Huang, "Discrete-time sliding mode control for deployment of tethered space robot with only length and angle measurement," *IEEE Trans. Aerosp. Electron. Syst.*, vol. 56, no. 1, pp. 585–596, Feb. 2020.

[3] B. Xiao, L. Cao, S. Xu, and L. Liu, "Robust tracking control of robot manipulators with actuator faults and joint velocity measurement uncertainty," *IEEE/ASME Trans. Mechatronics*, vol. 25, no. 3, pp. 1354–1365, Jun. 2020.

[4] R. Middletone and G. Goodwin, "Adaptive computed torque control for rigid link manipulators," in *Proc. 25th IEEE Conf. Decis. Control*, Athens, Greece, Dec. 1986, pp. 68–73.

[5] J. H. Oh and J. S. Lee, "Control of flexible joint robot system by backstepping design approach," in *Proc. IEEE Int. Conf. Robot. Autom.*, Albuquerque, NM, USA, Apr. 1997, pp. 3435–3440.

[6] B. Brahmi, M. Saad, C. Ochoa-Luna, M. H. Rahman, and A. Brahmi, "Adaptive tracking control of an exoskeleton robot with uncertain dynamics based on estimated time-delay control," *IEEE/ASME Trans. Mechatronics*, vol. 23, no. 2, pp. 575–585, Apr. 2018.

[7] H. Wang, Y. Pan, S. Li, and H. Yu, "Robust sliding mode control for robots driven by compliant actuators," *IEEE Trans. Control Syst. Technol.*, vol. 27, no. 3, pp. 1259–1266, May 2019.

[8] Y. Feng, X. Yu, and Z. Man, "Non-singular terminal sliding mode control of rigid manipulators," *Automatica*, vol. 38, no. 12, pp. 2159–2167, 2002.

[9] Y. Pan, H. Wang, X. Li, and H. Yu, "Adaptive command-filtered backstepping control of robot arms with compliant actuators," *IEEE Trans. Control Syst. Technol.*, vol. 26, no. 3, pp. 1149–1156, May 2018.

[10] M. Joo Er and S. Hong Chin, "Hybrid adaptive fuzzy controllers of robot manipulators with bounds estimation," *IEEE Trans. Ind. Electron.*, vol. 47, no. 5, pp. 1151–1160, Oct. 2000.

[11] R. J. Wai and R. Muthusamy, "Fuzzy-neural-network inherited sliding-mode control for robot manipulator including actuator dynamics," *IEEE Trans. Neural Netw. Learn. Syst.*, vol. 24, no. 2, pp. 274–287, Feb. 2013.

[12] D. Q. Mayne, J. B. Rawlings, C. V. Rao, and P. O. M. Scokaert, "Constrained model predictive control: Stability and optimality," *Automatica*, vol. 36, no. 6, pp. 789–814, 2000.

[13] H. Michalska and D. Q. Mayne, "Robust receding horizon control of constrained nonlinear systems," *IEEE Trans. Autom. Control*, vol. AC-38, no. 11, pp. 1623–1633, Nov. 1993.

[14] L. Grüne, "Economic receding horizon control without terminal constraints," *Automatica*, vol. 49, no. 3, pp. 725–734, 2013.

[15] M. B. Kane, J. P. Lynch, and J. Scruggs, "Run-time efficiency of bilinear model predictive control using variational methods, with applications to hydronic cooling," *IEEE/ASME Trans. Mechatronics*, vol. 24, no. 2, pp. 718–728, Apr. 2019.

[16] D. Tavernini, M. Metzler, P. Gruber, and A. Sorniotti, "Explicit nonlinear model predictive control for electric vehicle traction control," *IEEE Trans. Control Syst. Technol.*, vol. 27, no. 4, pp. 1438–1451, Jul. 2019.

[17] L. Grüne, "NMPC without terminal constraints," *IFAC Proc. Vol.*, vol. 45, no. 17, pp. 1–13, 2012.

[18] J. Kohler, M. A. Müller, and F. Allgöwer, "Nonlinear reference tracking: An economic model predictive control perspective," *IEEE Trans. Autom. Control*, vol. 64, no. 1, pp. 254–269, Jan. 2019.

[19] J. Köhler, R. Soloperto, M. A. Müller, and F. Allgöwer, "A computationally efficient robust model predictive control framework for uncertain nonlinear systems," *IEEE Trans. Autom. Control*, vol. 66, no. 2, pp. 794–801, Feb. 2021.

[20] J. Seo, S. Lee, J. Lee, and J. Choi, "Nonaffine helicopter control design and implementation based on a robust explicit nonlinear model predictive control," *IEEE Trans. Control Syst. Technol.*, early access, Apr. 6, 2021, doi: 10.1109/TCST.2021.3069106.

[21] L. Hewing, J. Kabzan, and M. N. Zeilinger, "Cautious model predictive control using Gaussian process regression," *IEEE Trans. Control Syst. Technol.*, vol. 28, no. 6, pp. 2736–2743, Nov. 2020.

[22] X. Xu, H. Chen, C. Lian, and D. Li, "Learning-based predictive control for discrete-time nonlinear systems with stochastic disturbances," *IEEE Trans. Neural Netw. Learn. Syst.*, vol. 29, no. 12, pp. 6202–6213, Dec. 2018.

[23] J. Huang, Y. Cao, C. Xiong, and H.-T. Zhang, "An echo state Gaussian process-based nonlinear model predictive control for pneumatic muscle actuators," *IEEE Trans. Autom. Sci. Eng. (from July 2004)*, vol. 16, no. 3, pp. 1071–1084, Jul. 2019.

[24] J. M. Manzano, D. Limon, D. Muñoz de la Peña, and J.-P. Calliess, "Robust learning-based MPC for nonlinear constrained systems," *Automatica*, vol. 117, Jul. 2020, Art. no. 108948.

[25] P. O. M. Scokaert and D. Q. Mayne, "Min-max feedback model predictive control for constrained linear systems," *IEEE Trans. Autom. Control*, vol. 43, no. 8, pp. 1136–1142, Aug. 1998.

[26] O. Khan, G. Mustafa, A. Q. Khan, M. Abid, and M. Ali, "Fault-tolerant robust model-predictive control of uncertain time-delay systems subject to disturbances," *IEEE Trans. Ind. Electron.*, vol. 68, no. 11, pp. 11400–11408, Nov. 2021.

[27] M. Rubagotti, D. M. Raimondo, A. Ferrara, and L. Magni, "Robust model predictive control with integral sliding mode in continuous-time sampled-data nonlinear systems," *IEEE Trans. Autom. Control*, vol. 56, no. 3, pp. 556–570, Mar. 2011.

[28] F. Bayat, "Model predictive sliding control for finite-time three-axis spacecraft attitude tracking," *IEEE Trans. Ind. Electron.*, vol. 66, no. 10, pp. 7986–7996, Oct. 2019.

[29] N. Ghahramani and F. Towhidkhah, "Constrained incremental predictive controller design for a flexible joint robot," *ISA Trans.*, vol. 48, pp. 321–326, Jul. 2009.

[30] D. L. Marruedo, T. Alamo, and E. F. Camacho, "Input-to-state stable MPC for constrained discrete-time nonlinear systems with bounded additive uncertainties," in *Proc. 41st IEEE Conf. Decis. Control*, Las Vegas, NV, USA, Dec. 2002, pp. 4619–4624.

[31] S. Heshmati-Alamdari, G. C. Karras, P. Marantos, and K. J. Kyriakopoulos, "A robust predictive control approach for underwater robotic vehicles," *IEEE Trans. Control Syst. Technol.*, vol. 28, no. 6, pp. 2352–2363, Nov. 2020.

[32] Z. Li and J. Sun, "Disturbance compensating model predictive control with application to ship heading control," *IEEE Trans. Control Syst. Technol.*, vol. 20, no. 1, pp. 257–265, Jan. 2012.

[33] L. Grüne and J. Pannek, *Nonlinear Model Predictive Control: Theory and Algorithms*. London, U.K.: Springer, 2017.

[34] L. Grüne and V. G. Palma, "Robustness of performance and stability for multistep and updated multistep MPC schemes," *Discrete Continuous Dyn. Syst.*, vol. 35, no. 9, pp. 4385–4414, 2015.

[35] L. Grüne and V. G. Palma, "On the benefit of re-optimization in optimal control under perturbations," in *Proc. 21st Int. Symp. Math. Theory Netw. Syst.*, Groningen, The Netherlands, Jul. 2014, pp. 439–446.

[36] K. Youcef-Toumi and S.-T. Wu, "Input/output linearization using time delay control," *J. Dyn. Syst., Meas., Control*, vol. 114, no. 1, pp. 10–19, Mar. 1992.

[37] T. C. Hsia and L. S. Gao, "Robot manipulator control using decentralized linear time-invariant time-delayed joint controllers," in *Proc. IEEE Int. Conf. Robot. Autom.*, Cincinnati, OH, USA, May 1990, pp. 2070–2075.

[38] J. Lee, H. Dallali, M. Jin, D. G. Caldwell, and N. G. Tsagarakis, "Robust and adaptive dynamic controller for fully-actuated robots in operational space under uncertainties," *Auton. Robots*, vol. 43, no. 4, pp. 1023–1040, Apr. 2019.

[39] M. Jin, J. Lee, and N. G. Tsagarakis, "Model-free robust adaptive control of humanoid robots with flexible joints," *IEEE Trans. Ind. Electron.*, vol. 64, no. 2, pp. 1706–1715, Feb. 2017.

[40] J. Baek, M. Jin, and S. Han, "A new adaptive sliding-mode control scheme for application to robot manipulators," *IEEE Trans. Ind. Electron.*, vol. 63, no. 6, pp. 3628–3637, Jun. 2016.

[41] R. Hayat and M. Buss, "Model identification for robot manipulators using regressor-free adaptive control," in *Proc. UKACC 11th Int. Conf. Control*, Belfast, U.K., Aug. 2016, pp. 1–7.

[42] S. Roy, S. B. Roy, J. Lee, and S. Baldi, "Overcoming the underestimation and overestimation problems in adaptive sliding mode control," *IEEE/ASME Trans. Mechatronics*, vol. 24, no. 5, pp. 2031–2039, Oct. 2019.

[43] W. M. Grimm, "Robot non-linearity bounds evaluation techniques for robust control," *Int. J. Adapt. Control Signal Process.*, vol. 4, no. 6, pp. 501–522, Nov. 1990.

[44] M. Jin, J. Lee, P. H. Chang, and C. Choi, "Practical nonsingular terminal sliding-mode control of robot manipulators for high-accuracy tracking control," *IEEE Trans. Ind. Electron.*, vol. 56, no. 9, pp. 3593–3601, Sep. 2009.

[45] J. Lee, N. Deshpande, D. G. Caldwell, and L. S. Mattos, "Microscale precision control of a computer-assisted transoral laser microsurgery system," *IEEE/ASME Trans. Mechatronics*, vol. 25, no. 2, pp. 604–615, Apr. 2020.

[46] C. Shen, Y. Shi, and B. Buckham, "Trajectory tracking control of an autonomous underwater vehicle using Lyapunov-based model predictive control," *IEEE Trans. Ind. Electron.*, vol. 65, no. 7, pp. 5796–5805, Jul. 2018.

[47] S. Rastegarpour, S. Gros, and L. Ferrarini, "MPC approaches for modulating air-to-water heat pumps in radiant-floor buildings," *Control Eng. Pract.*, vol. 95, Feb. 2020, Art. no. 104209.
[48] Y. Fang and A. Armaou, "Nonlinear model predictive control using a bilinear Carleman linearization-based formulation for chemical processes," in *Proc. Amer. Control Conf. (ACC)*, Chicago, IL, USA, Jul. 2015, pp. 5629–5634.
[49] J. Kohler, M. A. Müller, and F. Allgower, "A nonlinear model predictive control framework using reference generic terminal ingredients," *IEEE Trans. Autom. Control*, vol. 65, no. 8, pp. 3576–3583, Aug. 2020.
[50] D. Limon, A. Ferramosca, I. Alvarado, and T. Alamo, "Nonlinear MPC for tracking piece-wise constant reference signals," *IEEE Trans. Autom. Control*, vol. 63, no. 11, pp. 3735–3750, Nov. 2018.
[51] G. F. Franklin, J. D. Powell, and M. Workman, *Digital Control of Dynamic Systems*, 3rd ed. Menlo Park, CA, USA: Addison-Wesley, 1998.
[52] Z.-P. Jiang and Y. Wang, "Input-to-state stability for discrete-time nonlinear systems," *Automatica*, vol. 37, no. 6, pp. 857–869, Jun. 2001.
[53] Z. Zhang, M. Leibold, and D. Wollherr, "Integral sliding-mode observer-based disturbance estimation for Euler–Lagrangian systems," *IEEE Trans. Control Syst. Technol.*, vol. 28, no. 6, pp. 2377–2389, Nov. 2020.
[54] H. J. Ferreau, C. Kirches, A. Potschka, H. G. Bock, and M. Diehl, "qpOASES: A parametric active-set algorithm for quadratic programming," *Math. Program. Comput.*, vol. 6, no. 4, pp. 327–363, 2014.
[55] G. R. Cho, P. H. Chang, S. H. Park, and M. Jin, "Robust tracking under nonlinear friction using time-delay control with internal model," *IEEE Trans. Control Syst. Technol.*, vol. 17, no. 6, pp. 1406–1414, Nov. 2009.
[56] P. Falugi and D. Q. Mayne, "Getting robustness against unstructured uncertainty: A tube-based MPC approach," *IEEE Trans. Autom. Control*, vol. 59, no. 5, pp. 1290–1295, May 2014.
[57] U. Rosolia and F. Borrelli, "Learning model predictive control for iterative tasks. A data-driven control framework," *IEEE Trans. Autom. Control*, vol. 63, no. 7, pp. 1883–1896, Jul. 2018.
[58] L. Hewing, K. P. Wabersich, M. Menner, and M. N. Zeilinger, "Learning-based model predictive control: Toward safe learning in control," *Annu. Rev. Control, Robot., Auto. Syst.*, vol. 3, no. 1, pp. 269–296, May 2020.
[59] H. J. Wabersich, L. Hewing, A. Carron, and M. N. Zeilinger, "Probabilistic model predictive safety certification for learning-based control," *IEEE Trans. Autom. Control*, vol. 67, no. 1, pp. 176–188, Jan. 2022.

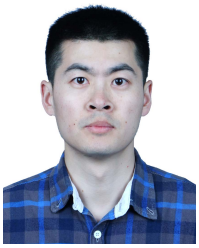

Yongchao Wang received the M.Sc. degree in control science and engineering from Xidian University, Xi'an, China, in 2016. He is currently pursuing the Ph.D. degree with the Chair of Automatic Control Engineering, Technical University of Munich, Munich, Germany.

He is also a Research Associate with the Chair of Automatic Control Engineering, Technical University of Munich. His research interests include adaptive control, robust nonlinear control, optimal control, backstepping, and robotics.

Marion Leibold (Member, IEEE) received the Diploma degree in applied mathematics and the Ph.D. degree in motion planning and control of legged robots from the Faculty of Electrical Engineering and Information Technology, Technical University of Munich, Munich, Germany, in 2002 and 2007, respectively.

She is currently a Senior Researcher with the Chair of Automatic Control Engineering, Faculty of Electrical Engineering and Information Technology, Technical University of Munich. Her research interests include optimal control and nonlinear control theory, and the applications to robotics.

Jinoh Lee (Senior Member, IEEE) received the B.S. degree *(summa cum laude)* in mechanical engineering from Hanyang University, Seoul, South Korea, in 2003, and the M.Sc. and Ph.D. degrees in mechanical engineering from the Korea Advanced Institute of Science and Technology, Daejeon, South Korea, in 2012.

He held a post-doctoral position at the Department of Advanced Robotics, Istituto Italiano di Tecnologia (IIT), Genoa, Italy, from 2012 to 2017, where he was a Research Scientist from 2017 to 2020. He is currently a Research Scientist with the Institute of Robotics and Mechatronics, German Aerospace Center (DLR), Weßling, Germany. His professional is about robotics and control engineering, which include manipulation of highly redundant robots such as dual-arm and humanoids, robust control of nonlinear systems, and compliant robotic system control for safe human–robot interaction.

Dr. Lee is a member of the IEEE Robotics and Automation, the IEEE Control Systems, and the IEEE Industrial Electronics Societies. He is also a Senior Editor of the IROS Conference Paper Review Board (CPRB).

Wenyan Ye received the B.Sc. degree in control science and engineering from Fuzhou University, Fuzhou, China, and the Technical University of Kaiserslautern, Kaiserslautern, Germany in 2018, and the M.Sc. degree from the Technical University of Munich, Munich, Germany, in 2020. He is currently pursuing the Ph.D. degree with the Institute of Automatic Control, University of Kaiserslautern.

His research interests include model predictive control, backstepping, and robotics.

Jing Xie (Graduate Student Member, IEEE) received the B.Sc. degree in automation from Southwest Jiaotong University, Chengdu, China, in 2017. He is currently pursuing the M.Sc. degree with the Chair of Automatic Control Engineering, Technical University of Munich, Munich, Germany.

His research interests include robust model predictive control, optimal control, and learning-based model predictive control.

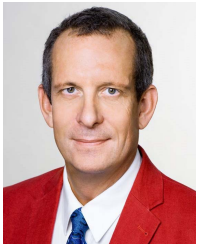

Martin Buss (Fellow, IEEE) received the Diploma Engineering degree in electrical engineering from the Technical University of Darmstadt, Darmstadt, Germany, in 1990, the D.Eng. degree in electrical engineering from The University of Tokyo, Tokyo, Japan, in 1994, and the Habilitation degree from the Technical University of Munich, Munich, Germany, in 2000.

In 1988, he was a Research Student with the Science University of Tokyo, Tokyo. From 1994 to 1995, he was a Post-Doctoral Researcher with the Department of System Engineering, Australian National University, Canberra, ACT, Australia. From 1995 to 2000, he was a Senior Research Assistant and a Lecturer with the Department of Electrical Engineering and Information Technology, Chair of Automatic Control Engineering, Technical University of Munich. From 2000 to 2003, he was a Full Professor, the Head of the Control Systems Group, and the Deputy Director of the Institute of Energy and Automation Technology, Faculty IV, Electrical Engineering and Computer Science, Technical University of Berlin, Berlin, Germany. Since 2003, he has been a Full Professor with the Chair of Automatic Control Engineering, Faculty of Electrical Engineering and Information Technology, Technical University of Munich, where he has been with the Medical Faculty since 2008. His research interests include automatic control, mechatronics, multimodal human–system interfaces, optimization, and hybrid systems.